The Diabatic and Nonlinear Aspects of the El Niño–Southern Oscillation: Implications for Its Past and Future Behavior

De-Zheng Sun

Cooperative Institute for Research in Environmental Sciences, University of Colorado at Boulder, Boulder, Colorado, USA
Earth System Research Laboratory, NOAA, Boulder, Colorado, USA

This chapter reviews recent advances in understanding the diabatic and nonlinear aspects of the El Niño–Southern Oscillation (ENSO). In particular, it reviews the research leading to the view that averaged over the decadal or longer time scales, ENSO acts as a basin-scale heat mixer in the tropical Pacific. This heat mixer regulates the long-term temperature difference between the surface water in the warm pool and the subsurface water constituting the equatorial undercurrent. When this temperature difference is externally forced to increase, the level of ENSO activity increases. Conversely, when this temperature difference is externally forced to decrease, the level of ENSO activity decreases. The time-mean effect of ENSO is to counteract the effect of external forcing on this temperature difference. This view of ENSO explains the recent trend in the level of ENSO activity in the instrumental record and sheds light on the behavior of ENSO in the past climates. The implied response in the level of ENSO activity to global warming, however, is at odds with the popular prediction by the state-of-the-art coupled climate models. Reasons for this discrepancy are explored. An inadequate sensitivity of the tropical hydrological cycle to sea surface temperature changes in the present coupled models is hypothesized as a possible factor responsible for the discrepancy.

1. INTRODUCTION

The steady increase in the CO_2 concentration and other man-made greenhouse gases in the atmosphere has caused due concern about the future of the state of the Earth's climate system [*Intergovernmental Panel on Climate Change*, 2007]. A question of prominence is what is the impact of the enhanced radiative heating in the atmosphere on the amplitude of natural variability in the climate system, in particular, those natural modes that have a global reach in causing climate anomalies [*Trenberth et al.*, 1998; *Glantz*, 2001; *McPhaden et al.*, 2006]. On this radar screen, the El Niño–Southern Oscillation (ENSO) figures prominently. ENSO not only causes anomalies in the seasonal mean temperature and precipitation worldwide [*Ropelewski and Halpert*, 1996; *Hoerling and Kumar*, 2003; *Huang and Wu*, 1989; *Wang et al.*, 2008; *Penland et al.*, this volume], it also affects the statistics of the extreme weather events, such as hurricanes/typhoons [*O'Brien et al.*, 1996] and midlatitude severe storms [*Barsugli et al.*, 1999; *Cayan et al.*, 2000; *Meehl et al.*, 2005]. Arguably, how the enhanced radiative heating due to the increasing CO_2 concentration in the atmosphere influences ENSO is one of the most important questions in the science of global climate change.

The most sophisticated tools to address this question are the state-of-the-art of the coupled models, but the biases in the simulated tropical Pacific climate of these models undermine confidence in the results from these models [*Sun et al.*, 2006; *Lin*, 2007; *Guilyardi et al.*, 2009; *Sun et al.*, 2009]. The complexity of these models also hinders understanding. The

Climate Dynamics: Why Does Climate Vary?
Geophysical Monograph Series 189

10.1029/2009GM000865

original theoretical framework developed to explain ENSO as a climate anomaly growing and decaying about a prescribed mean climate state [e.g., *Zebiak and Cane*, 1987] has shed light onto this important question [*Clement et al.*, 1996; *Cane et al.*, 1997]. Because the Zebiak and Cane (Z-C) model is an anomaly model and does not have an explicit heat budget for the subsurface ocean, the response of this model to an increase in the radiative heating is subject to question [*Cane*, 2004]. The Z-C model also left the feedback from ENSO onto the mean climate unaddressed.

This chapter attempts to provide a more systematic examination of the relationship of ENSO with radiative heating over the Pacific Ocean and to assess and delineate the collective effects of ENSO on the mean state. Because of the length restriction, the material reviewed will be focused on the research by the author and his collaborators. The goal is to present an extended picture of ENSO that not only reaffirms the importance of the dynamical coupling, the Bjerknes feedback, in giving rise to this important phenomenon (see review by *Neelin et al.* [1998]) but also highlights a fundamental

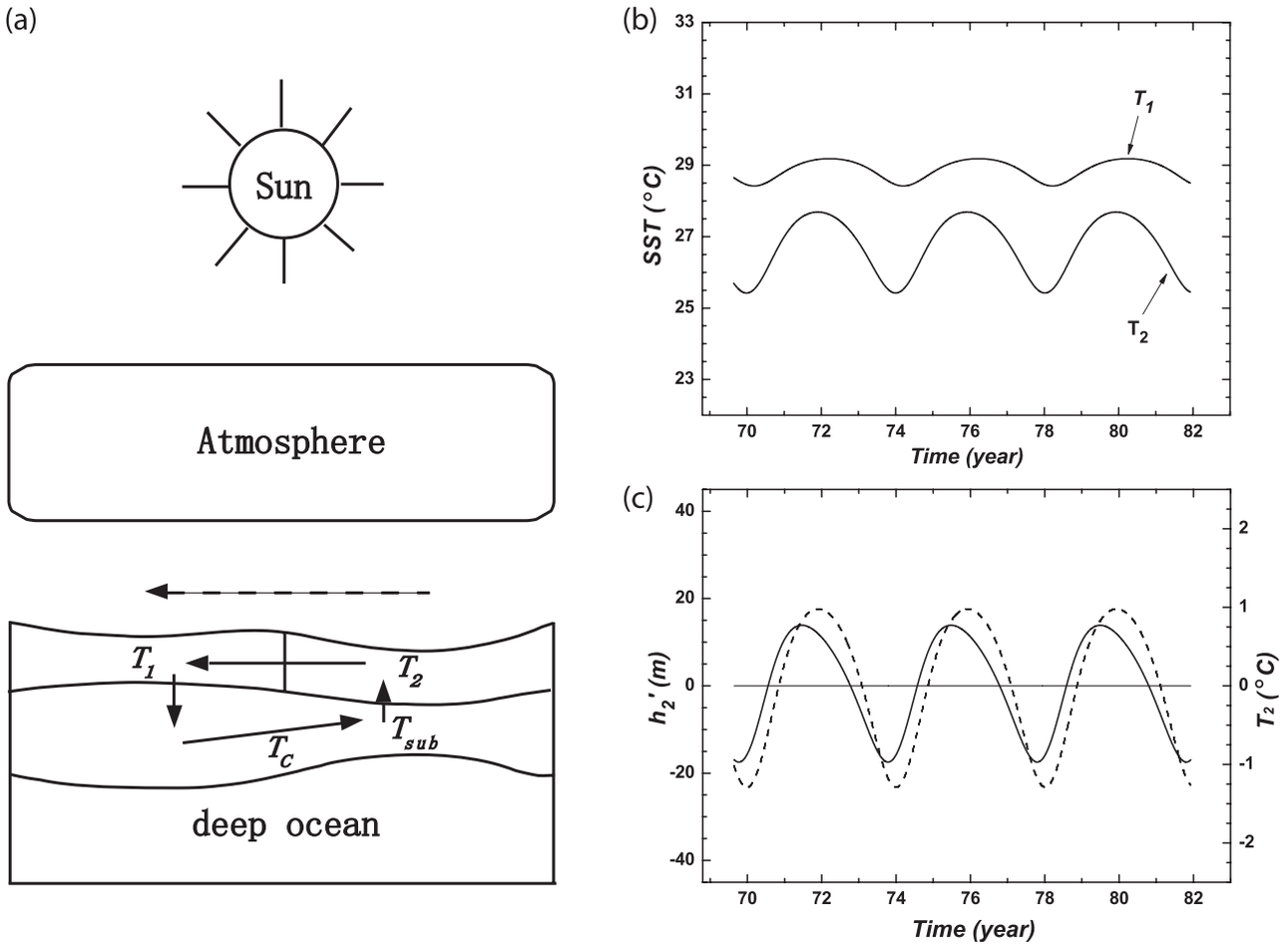

Figure 1. (a) Schematic diagram for the coupled model. Solid arrows represent the zonal branch of the equatorial wind-driven circulation constituted by the upwelling in the east Pacific, the westward surface drift, and the equatorial undercurrent. The thermodynamical effect of the atmosphere is to heat the ocean to a zonally uniform SST (T_w) if not opposed by ocean transport [see *Sun*, 2000, equations (6) and (7)]. (T_w has been called the radiative convective equilibrium SST and may be regarded as the tropical maximum SST or the SST of the warm pool). T_c represents the characteristic temperature of the equatorial undercurrent. T_{sub} is the temperature of the water that actually enters the surface mixed layer in the eastern Pacific. The dashed arrow represents the surface winds. (b and c) Oscillations at $T_w = 29.5°\text{C}$, a value corresponding to the maximum SST of the observed climate: variations of T_1 and T_2 (Figure 1b) and h_2 (anomaly of the thermocline depth in the eastern Pacific) (Figure 1c). The dashed line is anomalies of T_2.

force that sets the background stage for this positive feedback to operate on, the meridional differential heating over the Pacific Ocean. This force destabilizes the coupled tropical ocean-atmosphere through its impact on the temperature difference between the warm pool sea surface temperature (SST) (T_w) and the equatorial thermocline water (T_c) [*Sun*, 2003; *Sun et al.*, 2004]. More importantly, it will be shown that by repeatedly sloshing the tropical upper ocean water, ENSO acts as basin-scale heat mixer that regulates the long-term mean value of this temperature contrast [*Sun and Zhang*, 2006; *Sun*, 2007].

This extended picture of ENSO suggests an interesting scenario for the response of ENSO to global warming. During the initial stage of global warming, $T_w - T_c$ is likely to increase because of the forcing from global warming. An elevated ENSO activity then ensues in response. During the late stage of global warming, however, $T_w - T_c$ is likely to decrease in response to the flux of warmer extratropical surface water to the subsurface of the equatorial Pacific. Then the level of ENSO activity may reduce. Do observational data support this scenario? Do the results from the state-of-the-art models support this scenario? If not, why? This chapter also attempts to provide some discussion about these questions that may be useful for further research.

This chapter is organized as follows. We first review the theoretical progress that has been made on the diabatic and nonlinear aspects of ENSO. We then present an analysis of the recent elevation of ENSO activity as a first test of the theory developed. We then review paleoclimate findings concerning the behavior of ENSO in the past climates and examine whether the past behavior of ENSO can be explained by the theoretical results. Finally, we discuss the simulations by the Intergovernmental Panel on Climate Change (IPCC) models of the response of ENSO to global warming and explain the discrepancies between the model simulations/projections and the theoretical predictions.

2. THEORETICAL ADVANCES

2.1. Insights From an Analytical Model

An analytical model was first used by the author to address the question of the impact of global warming on ENSO [*Sun*, 1997, 2000]. The coupled tropical Pacific ocean-atmosphere system is represented by a few boxes: one box for the atmosphere, two boxes for the surfaces oceans (the western and eastern surface Pacific), and one box for the subsurface upper ocean (Figure 1a). The thermodynamical effect of the atmosphere is to heat the ocean to a zonally uniform SST (T_w) if not opposed by ocean transport [see *Sun*, 2000, equations (6) and (7)]. (T_w has been called the radiative convective equilibrium SST and may be regarded as the tropical maximum SST or the SST of the warm pool.) The zonal wind stress is coupled to the zonal SST contrast [*Sun*, 2000, equation (8)]. The treatment of upper ocean dynamics is based on the recharge and discharge oscillator model of *Jin* [1996] but with zonal advection added [see *Sun*, 2000, equations (11), (12), (13), and (14)]. The reference temperature profile for the subsurface box is further assumed to be determined by a balance between the surface heating from above and the cooling from upwelling of cold water from below. With realistic parameters, the model simulates the essential aspects

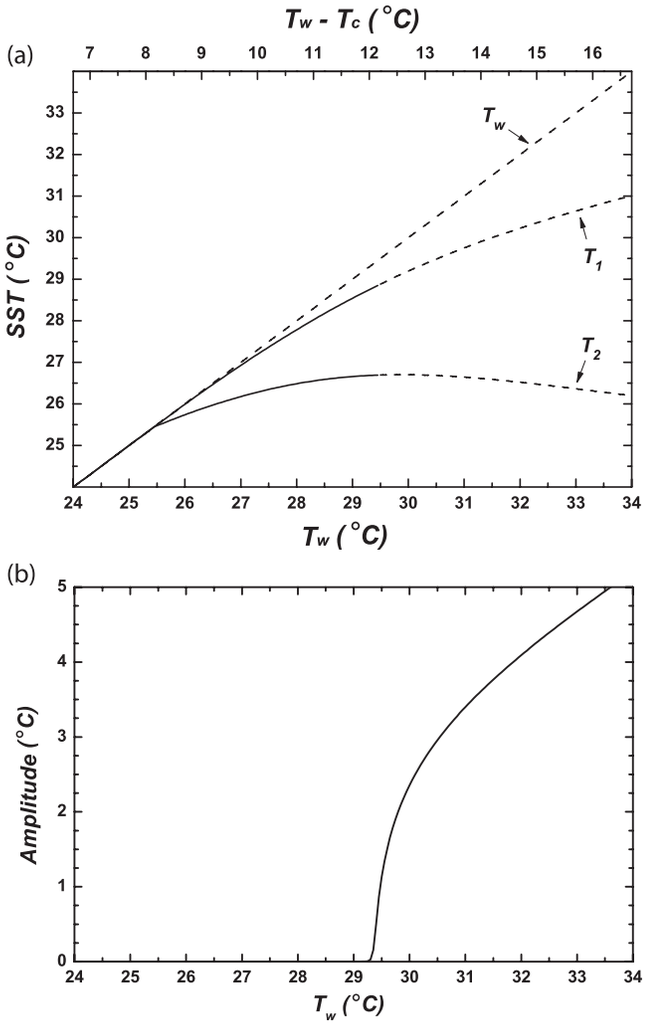

Figure 2. (a) Equilibrium solutions of the coupled system as a function of T_w. The value for T_c is fixed at 17.3°C. The corresponding differences between T_w and T_c are also marked in Figure 2a. Dashed lines indicate that the solution exists but is unstable. (b) Amplitude of oscillation as a function of T_w. For more details, see *Sun* [1997].

of ENSO including the preferred period, the westward propagation of the SST anomalies, and the phase relationship between SST and the depth of the thermocline in the eastern Pacific (Figures 1b and 1c). The oscillation is not always regular in the model, depending on the strength of the zonal advection relative to the strength of the total upwelling, as noted by *Timmermann and Jin* [2002]. Whether ENSO may be more adequately described as a series of events or as a cycle was discussed by *Kessler* [2002]. The asymmetry of ENSO in this model depends on the reference temperature profile for the thermocline [*Sun*, 2000, equation (10)].

The advantage of using an analytical model is that the behavior of the model in the full range of its parameter space can be easily obtained. An exploration of the behavior in the full range of its parameter space reveals that the system does not have to oscillate. It does not even have to have substantial zonal SST contrast as we have observed today. The reason that we have zonal SST contrast and an oscillatory behavior is because the warm pool SST is sufficiently high relative to the temperature of the equatorial undercurrent. These insights are drawn from Figure 2a, which shows the equilibrium change of the area mean SST of the eastern and western Pacific as a function of T_w (or $T_w - T_c$ as T_c is kept fixed). Figure 2a shows that when the value of T_w is sufficiently low, there is no zonal SST contrast. As the value of T_w becomes progressively high, the system experiences a pitchfork bifurcation to create the zonal SST contrast and then a Hopf bifurcation to enter an oscillatory state. Once the system enters the oscillatory state, the amplitude of oscillation increases with further increases in T_w (Figure 2b).

Critical for the instability of the steady circulation, the onset of an oscillatory regime, is that the temperature of the up-

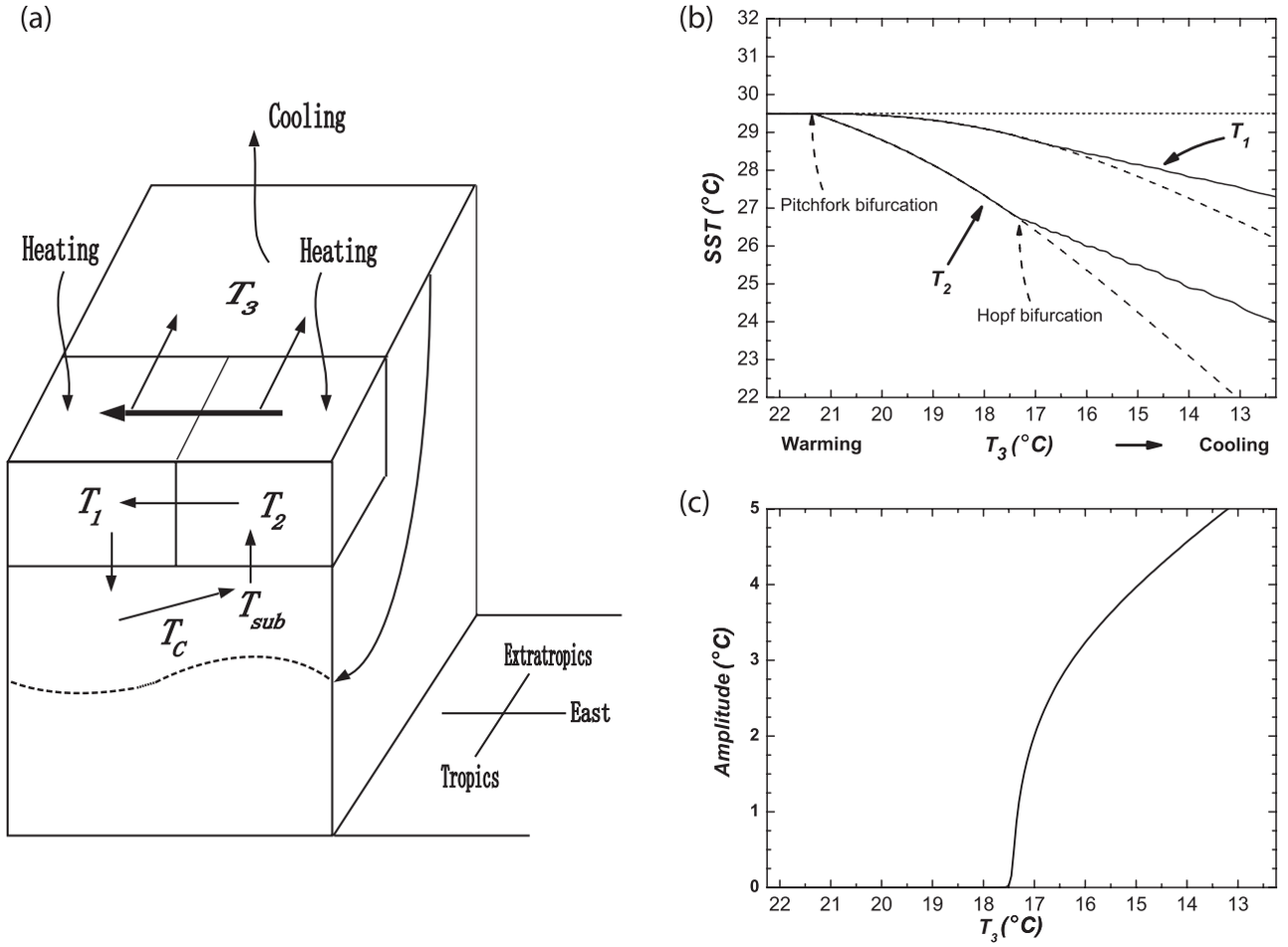

Figure 3. A schematic showing (a) the extended conceptual model, (b) equilibrium SST of the coupled system as a function of T_3, and (c) amplitude of the oscillation as a function of T_3. Warm pool temperature T_w is fixed at 29.5°C, as the value T_3 is varied.

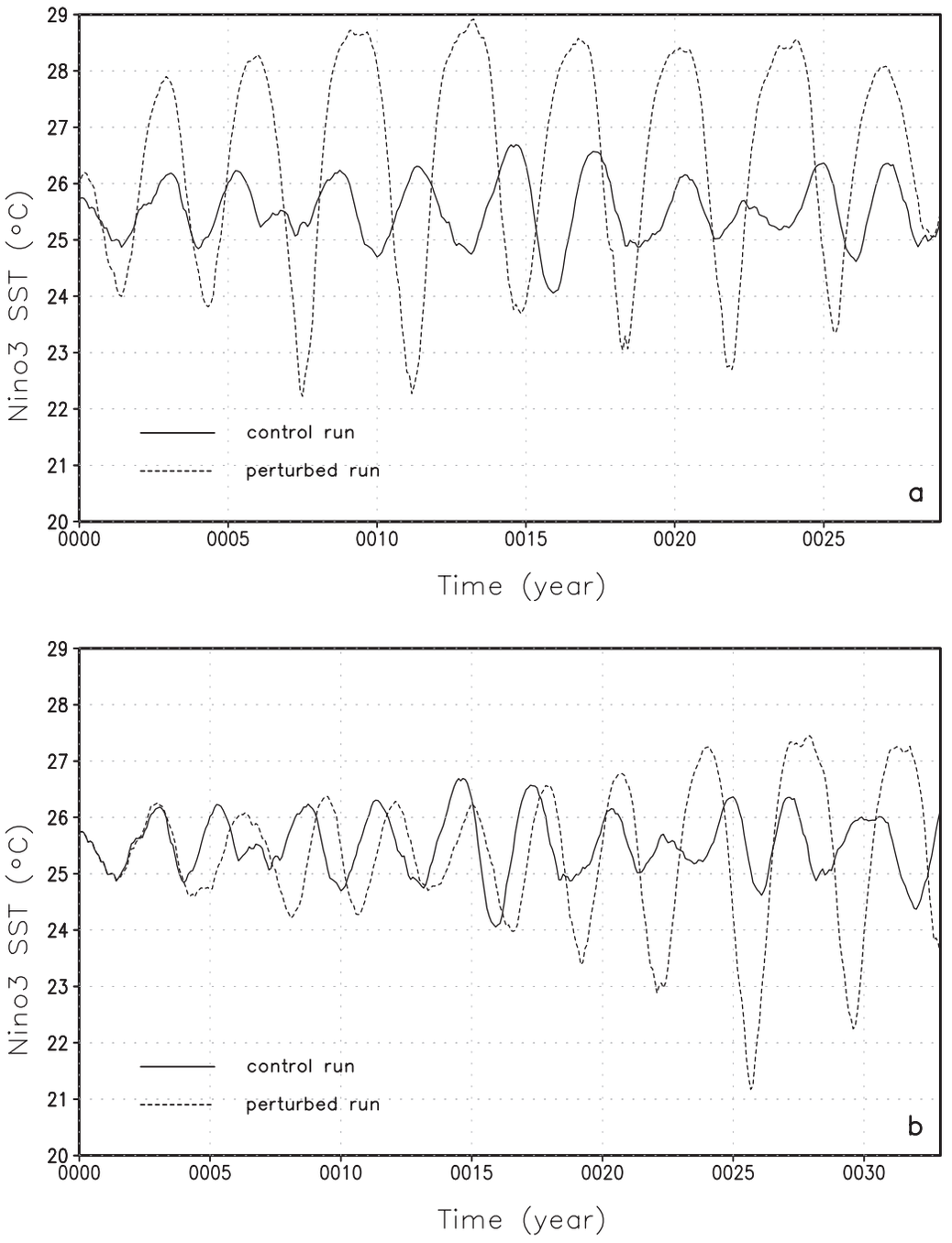

Figure 4. Response of ENSO to an increase in the (a) tropical heating and (b) extratropical cooling. Shown are time series of Niño 3 SST from a control run (solid line) and a perturbed run (dashed line) in which the restoring convective equilibrium temperature (SST_p) is either increased in to a higher value over the tropics (tropical heating case) or reduced to a lower value over the extraropics (extratropical cooling case). See *Sun et al.* [2004] for more details.

welled water depends strongly on the strength of the flow rate and that the flow rate (or the thermal forcing that drives the flow) is sufficiently large relative to the thermal and mechanical damping [*Sun*, 1997]. An analogous mechanism is responsible for the onset of oscillation in the Lorenz system [*Lorenz*, 1963], which is a low-order approximation of Rayleigh-Benard convection. Indeed, the oscillation in the present model does not have to be periodic; it can be chaotic [*Timmermann and Jin*, 2002]. Thus, the present explanation for the existence of ENSO may be regarded as more fundamental than the traditional explanation attributing the "turnaround" or the phase change of the ENSO to a delayed feedback from the subsurface ocean.

2.2. An Implied Role for the Extratropics

Further recognizing the water feeding the equatorial thermocline comes from the extratropics [*Pedlosky*, 1987; *McCreary and Lu*, 1994; *Liu et al.*, 1994], we have expanded the model to illustrate a possible role of extratropical warming/cooling from the high latitudes (Figure 3a). In this model, the temperature of the equatorial undercurrent (T_c) is directly linked to the extratropical SST (T_3). The equations governing the equatorial SST and the depth of the equatorial thermocline are the same as those for the model shown in Figure 1a. Figure 3b shows the mean SST as a function of the extratropical Pacific SST (T_3). (The dashed lines are for the equilibrium SST that becomes unstable.) Figure 3b shows that when the value of T_3 is sufficiently high relative to the value of T_w, there is no zonal SST contrast. As the value of T_3 becomes progressively lower, the system experiences a pitchfork bifurcation to create the zonal SST contrast and then a Hopf bifurcation to enter an oscillatory state. Once the system enters the oscillatory state, the amplitude of oscillation increases with further decreases in T_3 (Figure 3c). Thus, it appears that the extratropical cooling has the same impact as that from the tropical heating on the zonal SST contrast and the amplitude of ENSO.

2.3. Results From a Numerical Model

We then replaced the box model with the National Center for Atmospheric Research (NCAR) Pacific basin model, the primitive equation model of *Gent and Cane* [1989]. Details of the hybrid coupled model are provided by *Sun* [2003] and *Sun et al.* [2004]. The results from this more complicated model confirm the results from the analytical model (Figures 4a and 4b): either an increase in the tropical heating or an increase in the extratropical cooling may increase the amplitude of ENSO. Note that the impact from the extratropical cooling on the level of ENSO activity is not immediate but is delayed (Figure 4b). This is because it takes time for the cold surface water of the extratropical ocean to reach the equatorial subsurface via the subduction process [*Pedlosky*, 1987; *McCreary and Lu*, 1994; *Sun et al.*, 2004]. As in the box model, annual cycle is not included in this hybrid model.

2.4. Feedback From ENSO Onto the Mean State

The results from the hybrid model also reveal that ENSO changes may feed back onto the mean climate state (i.e., its background state), in particular, onto the difference between the warm pool SST (T_w) and the temperature of the equatorial undercurrent (T_c). Table 1 lists results from three pairs of experiments designed to contrast the response of T_w, T_c, and $T_w - T_c$ in response to an enhanced tropical heating between the case with ENSO and the case without ENSO. (The case

Table 1 Response of T_w, T_c, and $T_w - T_c$ to an Enhanced Tropical Heating With and Without ENSO[a]

Perturbation Type	Experiment Type	Change of T_w (°C)	Change of T_c (°C)	Change of $T_w - T_c$ (°C)
Pair I (5°S–5°N)	no ENSO	1.03	0.0050	1.02
	with ENSO	0.81	0.76	0.053
Pair II (10°S–10°N)	no ENSO	1.38	0.036	1.34
	with ENSO	0.97	0.83	0.14
Pair III (15°S–15°N)	no ENSO	0.95	0.24	0.71
	with ENSO	0.55	0.63	−0.085

[a]The definitions of T_w and T_c are the same as given by *Sun et al.* [2004]. The three pairs presented here differ in the meridional extent of the regions where an enhanced tropical heating is applied. Anomalous heating is confined to 5°S–5°N for pair I, 10°S–10°N for pair II, and 15°S–15°N for pair III. In all three cases, the increase in the radiative convective equilibrium SST (SST_p) peaks at the equator with a value of 2°C and then decreases with latitude following a cosine profile to zero at the specified latitudes (i.e., 5°, 10°, and 15°, respectively for the three cases). The last 23 years of a 27 year long run are used in the calculation for the case with ENSO. For the case without ENSO, the last 3 years of data of a 27 year long run are used in the calculation because there is little interannual variability in this case.

without ENSO refers to a case in which the equatorial ocean-atmosphere system is not dynamically coupled: the winds are constant.) In all three pairs, the response in $T_w - T_c$ to tropical heating is much reduced in the case of ENSO than in the case without ENSO.

Plate 1 provides a more detailed look of the response in the time-mean temperature of the equatorial upper ocean. Plates 1a and 1b show the equatorial temperature differences (5°S–5°N) between the control run and the perturbed run for the case without ENSO and for the case with ENSO, respectively. Without ENSO, the warming of the tropical ocean is essentially confined to the surface layer, with the response in the western Pacific being slightly deeper than in the eastern Pacific. With ENSO, the response extends to the thermocline. While the thermocline water is much warmer in the case with ENSO, the response at the surface western Pacific is reduced.

This feedback of ENSO as evident in Plate 1 is linked to the asymmetric response in the two phases of ENSO. Stronger La Niña is accompanied by stronger winds, which enables more heat to be pumped downward to the subsurface ocean, the western part of the ocean in particular in the equatorial region. Plate 2a shows the upper ocean temperature changes during La Niña events in response to the enhanced tropical heating. The thermocline is deeper in the western Pacific, consistent

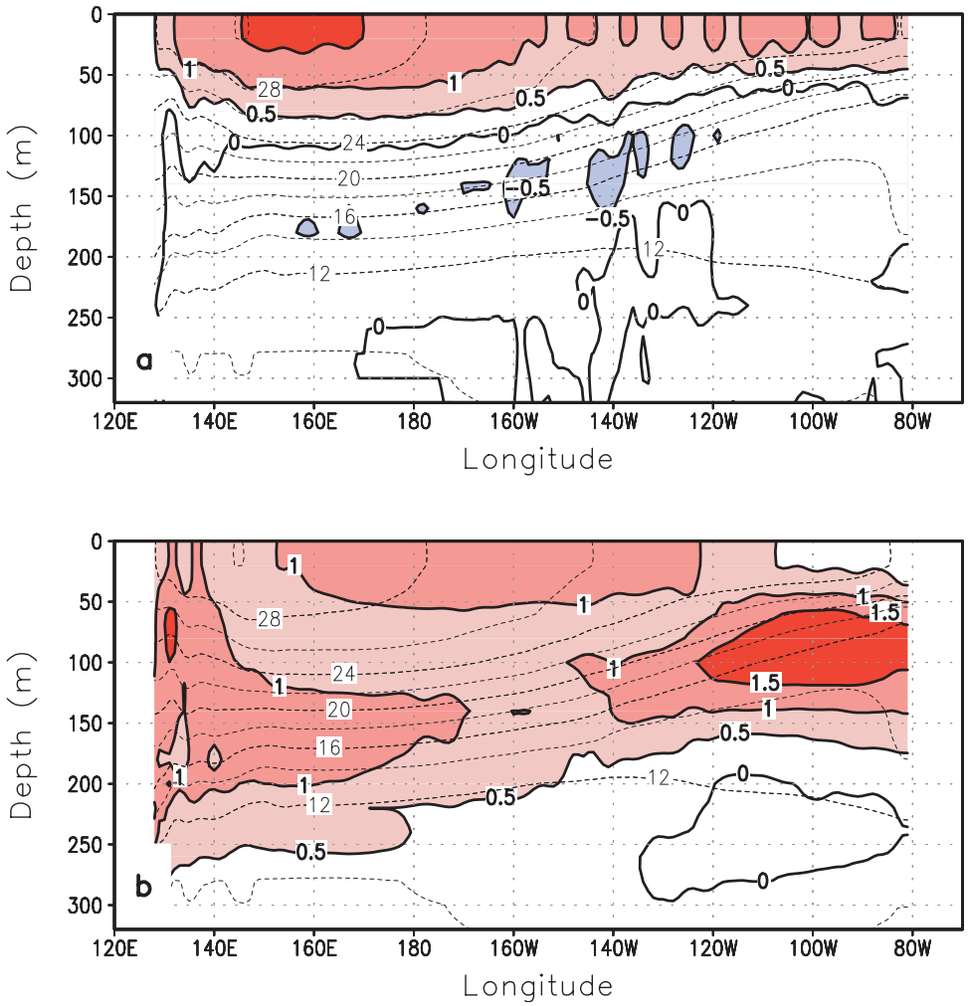

Plate 1. Time-mean equatorial upper ocean temperature response to an enhanced tropical heating for (a) the case without ENSO and (b) the case with ENSO. Shown are the results from experiments of pair II listed in Table 1. Data used for the calculations here are the same as used for obtaining changes in T_w and T_c in Table 1. The thin dashed contours indicate the mean isentropes of the control run.

with the stronger zonal winds. Plate 2b shows the temperature differences in the warm phase. Stronger El Niño events then warm the upper ocean in the central and eastern Pacific. Averaged over the cold and warm phases, the heat is "mixed" downward across the basin.

The feedback of ENSO onto the mean climate also shows up in the extratropical cooling experiments. A typical respone in the time-mean temperature of the equatorial upper ocean (5°S–5°N) to an enhanced extratropical cooling is shown in Figure 5a for the case without ENSO and in Figure 5b for the case with ENSO. Without ENSO, the equatorial thermocline water (T_c) is cooled by about 1°C by the imposed cooling over the subtropical surface ocean. The cooling of the equatorial ocean is largely confined to the subsurface; the cooling of the western Pacific SST (T_w) is negligible. With ENSO, the cooling of the thermocline water is reduced down to about 0.5°C while the cooling of the surface western Pacific is enhanced by about the same amount.

Figure 6 further shows a meridional section of the ocean temperature change at the central Pacific. Again, Figure 6a is the case without ENSO, and Figure 6b is for the case with ENSO. The role of subduction in carrying the cooling from the extratropics to the equatorial subsurface is evident in the case without ENSO. With ENSO, the equatorial region and the high latitudes appear to be disconnected, particularly in the Northern Hemisphere. This may provide an explanation

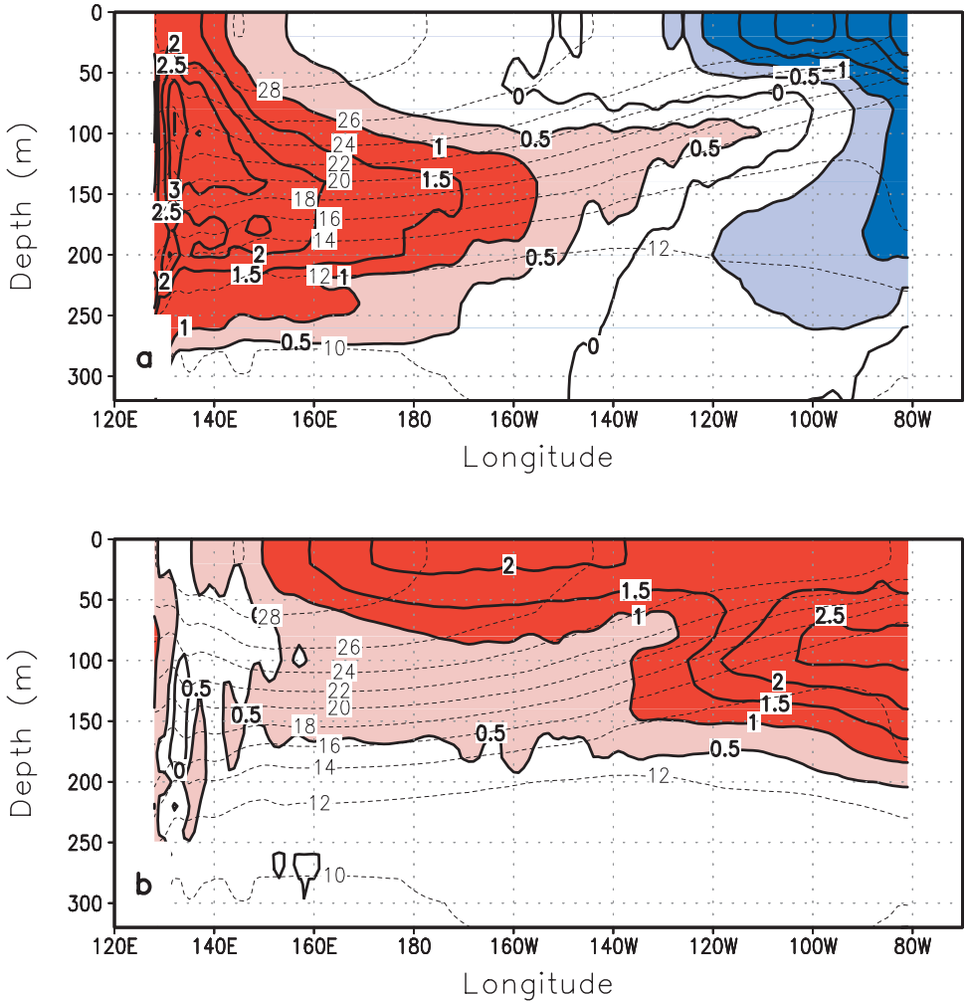

Plate 2. Differences in the equatorial upper ocean temperature between the perturbed run and the control run during the (a) La Niña phase (a) and (b) El Niño phase. The results are from pair II (see Table 1 footnote). The six cycles of the last 23 years of a 27 year long run are used in this calculation.

for why it is difficult to trace a decadal temperature anomaly in the real world all the way from the extratropics to the equatorial Pacific [*Deser et al.*, 1996; *Schneider et al.*, 1999]. The real world has recurrent occurrences of ENSO events, which effectively destroys the temperature anomalies on the decadal and longer time scales through effective mixing in the tropical Pacific. Therefore, the apparent disappearance of decadal temperature anomalies at the equatorial region in the observations does not suggest an ineffective extratropical influence over the level of ENSO activity.

This feedback of ENSO as evident in the cooling case again is linked to the asymmetric response in the two phases of ENSO. Plates 3a and 3b show the upper ocean temperature changes during La Niña events and the El Niño events, respectively. The cooling of the western Pacific occurs only in the warm phase, and the cooling of the eastern Pacific occurs only in the cold phase. Despite the imposed extratropical cooling, the eastern Pacific actually becomes warmer in the warm phase. Warming also occurs in the western Pacific during the cold phase.

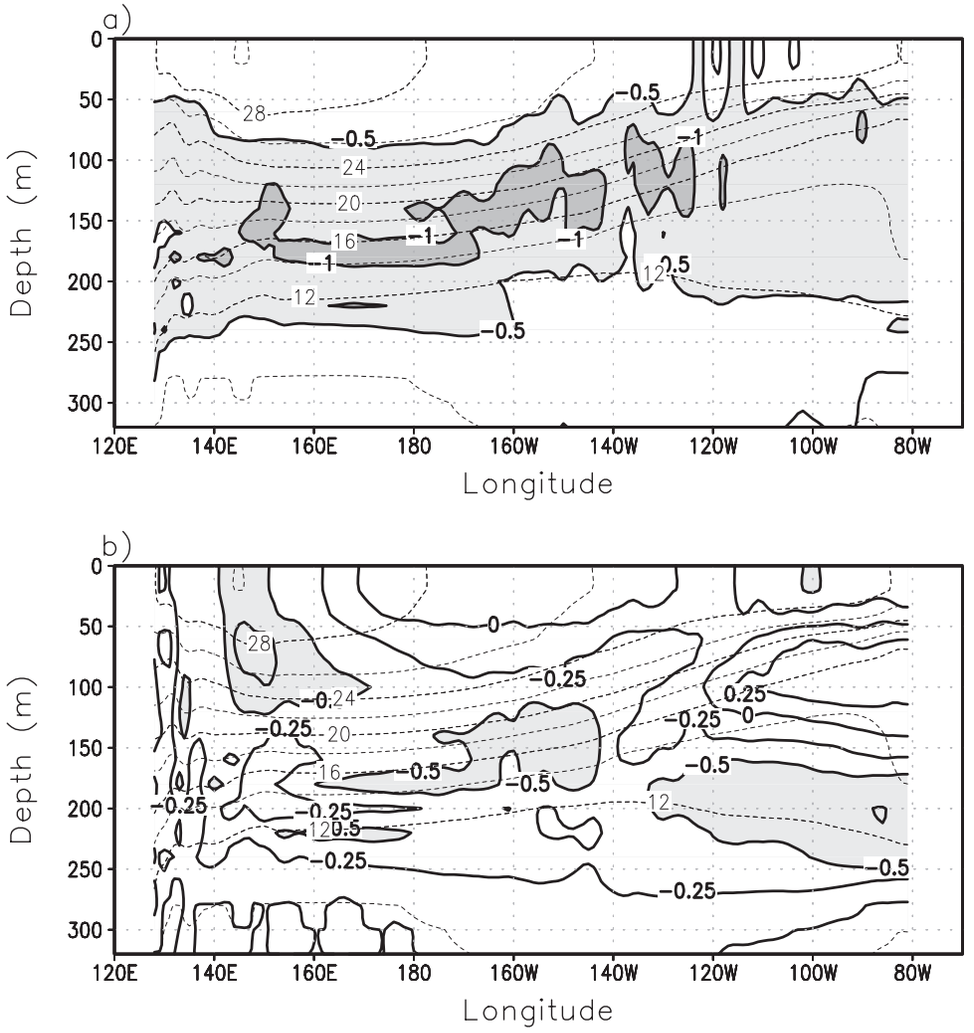

Figure 5. Time-mean equatorial upper ocean temperature response to an enhanced extratropical cooling (a) for the case without ENSO and (b) the case with ENSO. Anomalous extratropical cooling, a reduction in SST_p, starts at 10°S(N) and increases monotonically with latitude to a fixed value 1°C at 30°S(N). The last 3 years of data of a 27 year long run are used in the calculation for the case without ENSO. For the case with ENSO, the last 23 years of a 40 year long run are used. Not like the almost instantaneous response of ENSO to an increase in the tropical heating, there is a delay for the onset of the regime with stronger ENSO in response to an increase in extratropical cooling. Consequently, there is a need for a longer run to obtain a time series of Niño 3 SST that is representative of the regime.

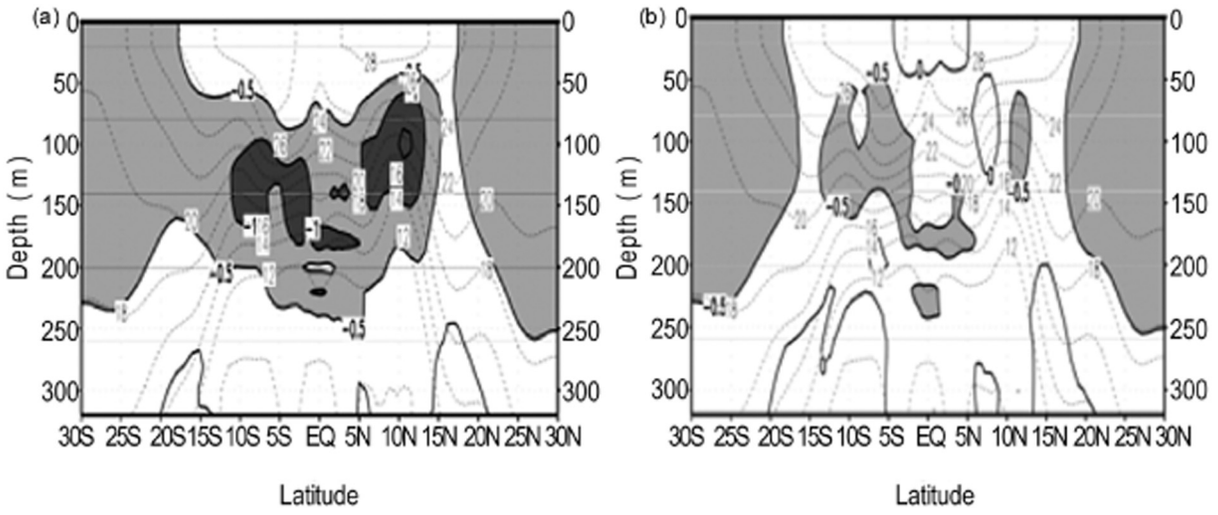

Figure 6. Response of the upper ocean temperature to extratropical cooling (a) with and (b) without ENSO. Shown are the zonal mean values.

The reduced sensitivity in $T_w - T_c$ to external forcing in the presence of ENSO underscores the fact that ENSO has a time-mean effect on the mean state. To further investigate the effects of ENSO on the mean climate, a pair of forced experiments is conducted. In one of them, the climatological surface wind stress over 1950–1999 is used, while in the other, the surface wind stress is climatological winds plus the interannual monthly anomalies (i.e., the actual monthly surface wind stress for the period 1950–1999). The long-term means of the surface wind stress in the two runs are thus identical. The two experiments also use the same restoring boundary conditions: the SST is restored to the same prescribed SST. The resulting equilibrium upper ocean temperatures are shown in Plates 4a and 4b. The case with fluctuating surface

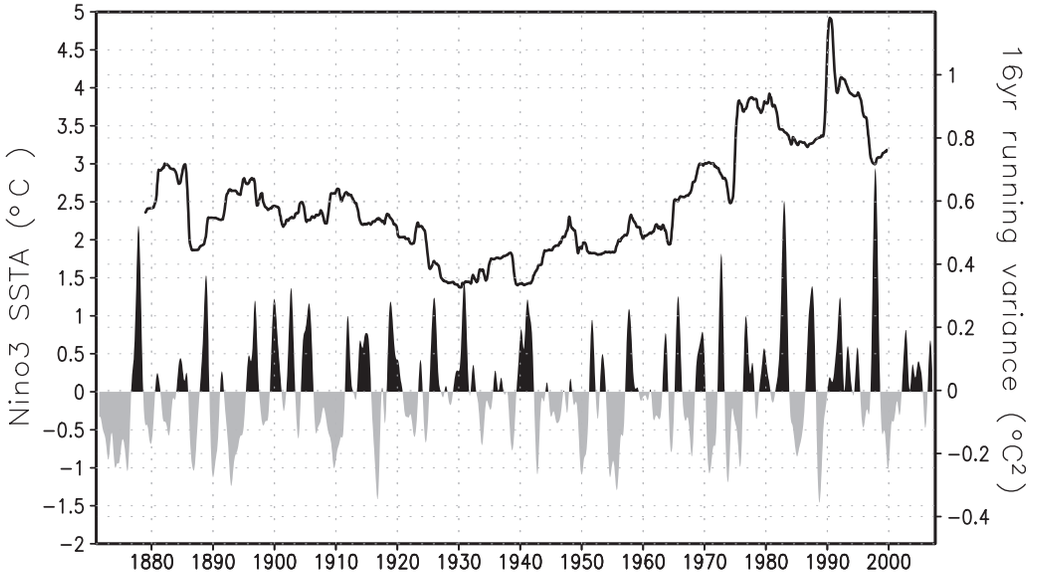

Figure 7. Niño 3 SST (anomalies) (bottom plot) and its variance (top plot). The variance of Niño 3 SST anomalies are obtained by sliding a moving window of a width of 16 years.

wind stress has a shallower warm pool but a thicker and more diffused thermocline. This effect of the fluctuating wind (the presence of ENSO) is shown more evidently in Plate 5a, which shows the difference in the equilibrium upper ocean temperature between these two phases. Plate 5a shows again that the role of ENSO is to cool the western Pacific warm pool but warm the subsurface thermocline water. We have also found that with the fluctuating part of the wind stress being magnified by 50%, the effect of ENSO on the mean upper ocean temperature is increased proportionally (Plate 5b). The exact mechanism for such a rectification effect is being investigated. Preliminary results suggest that the nonlinear "eddy" heating (i.e., the convergence of $\overline{V'T'}$, where V' and T' are the fluctuating part of the velocity and temperature, respectively, owing to ENSO, and the overbar denotes the time average over many cycles of ENSO) is a primary source for this effect. Note that here the "eddy" refers to part of the fluctuating part of the motion.

2.5. A Null Hypothesis for the Response of ENSO to Global Warming

The theoretical analysis suggests that collectively ENSO events act as a basin-scale heat exchanger that regulates the climatological temperature contrast between the warm pool (T_w) and the thermocline water (T_c). The level of ENSO

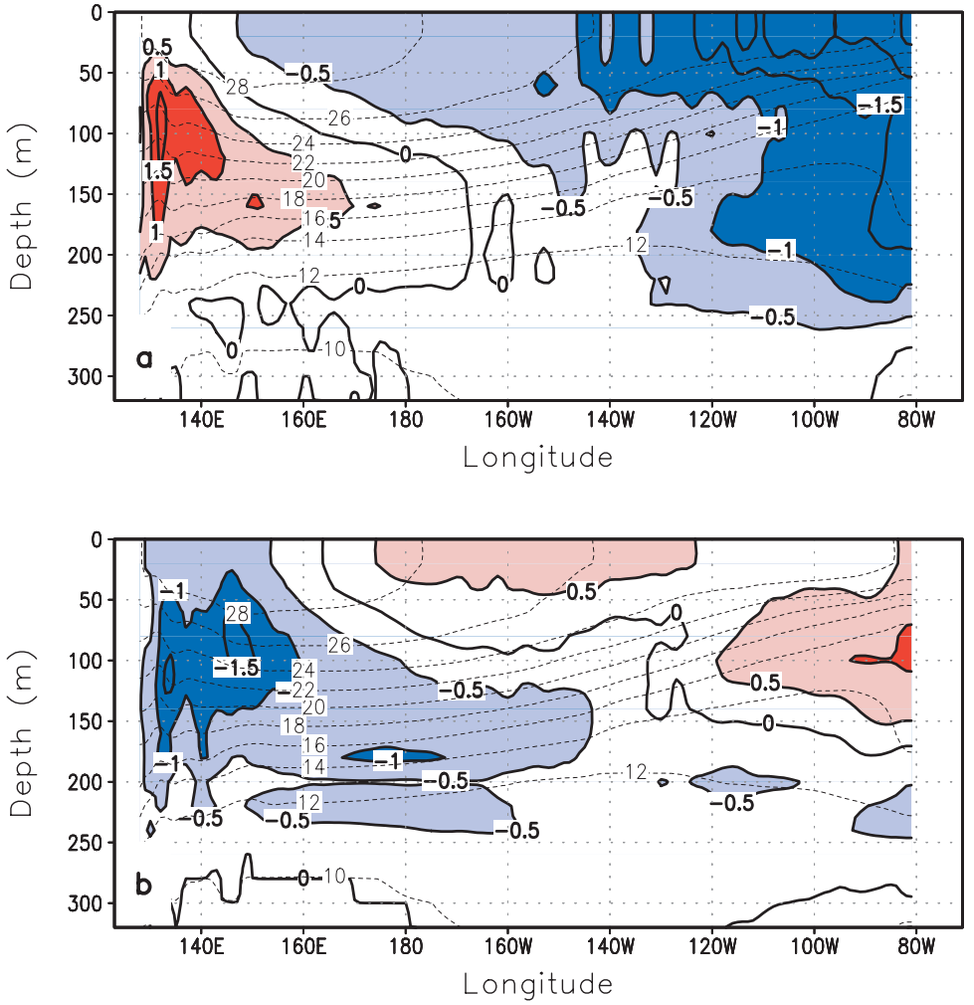

Plate 3. Differences in the equatorial upper ocean temperature between the perturbed run and the control run during the (a) La Niña phase and (b) El Niño phase for the enhanced extratropical cooling experiment. Data used are the same as for the case with ENSO in Plate 1.

activity may be proportional to the externally forced tendency in $T_w - T_c$. Global warming is likely to force $T_w - T_c$ to increase first because the surface feels the warming first. Eventually, however, because of the connection between the surface water over the extratropical Pacific and the subsurface water of the equatorial Pacific, the temperature of the subsurface water of the equatorial Pacific may increase at a rate more than the increase in the warm pool SST. Thus, the following scenario about how ENSO responds to global warming is raised: global warming would initially force an elevated ENSO activity, a more vigorous sloshing of the upper ocean water in the tropical Pacific. But the end result is likely the "death" of ENSO (or to put it more sanguinely, the creation of a permanent El Niño, a permanently warm state in the

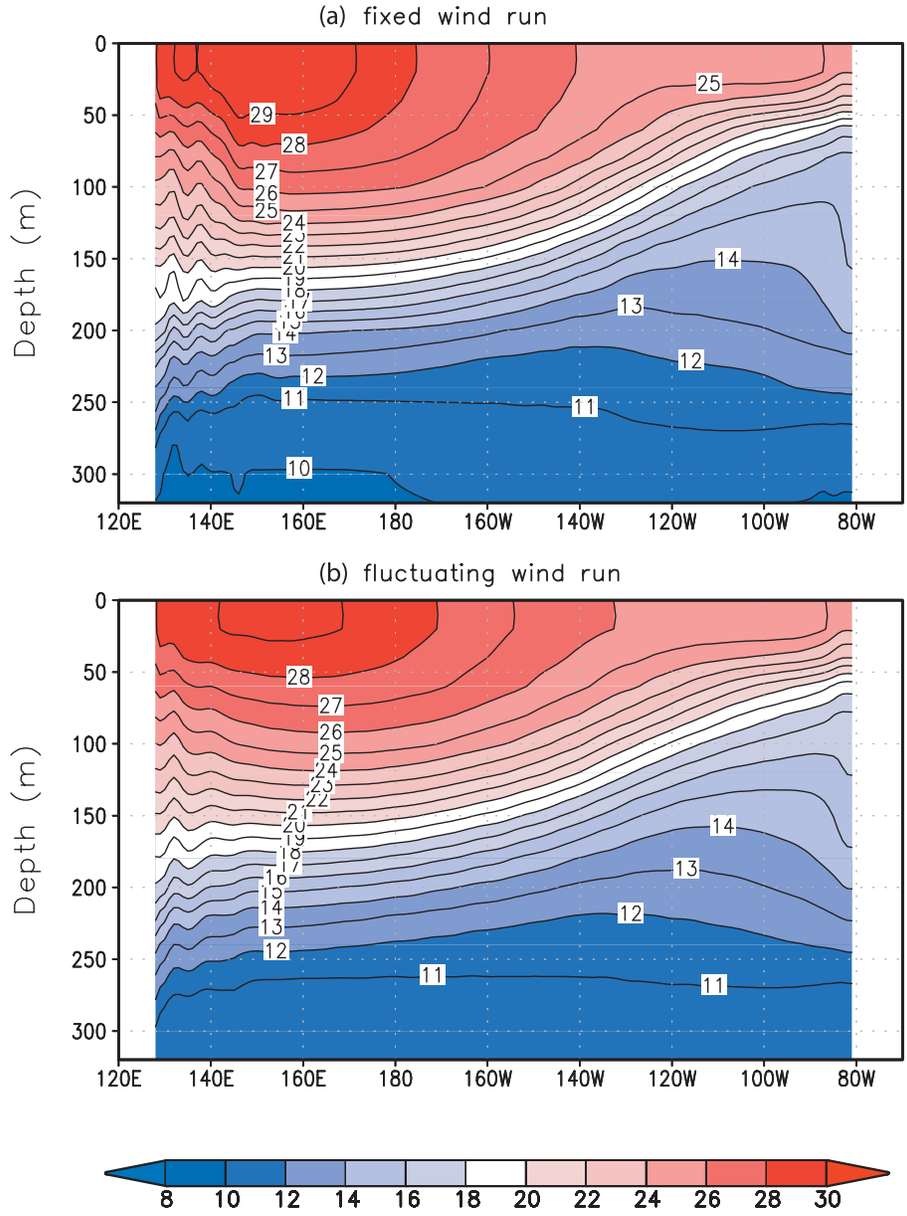

Plate 4. Equatorial upper ocean temperature from a run with (a) constant wind and (b) interannually varying wind. The time-mean wind stresses are the same as both runs (the 1950–1999 mean wind stress from the National Centers for Environmental Prediction), so are the thermal boundary conditions: both runs are restored to the same radiative convective equilibrium SST.

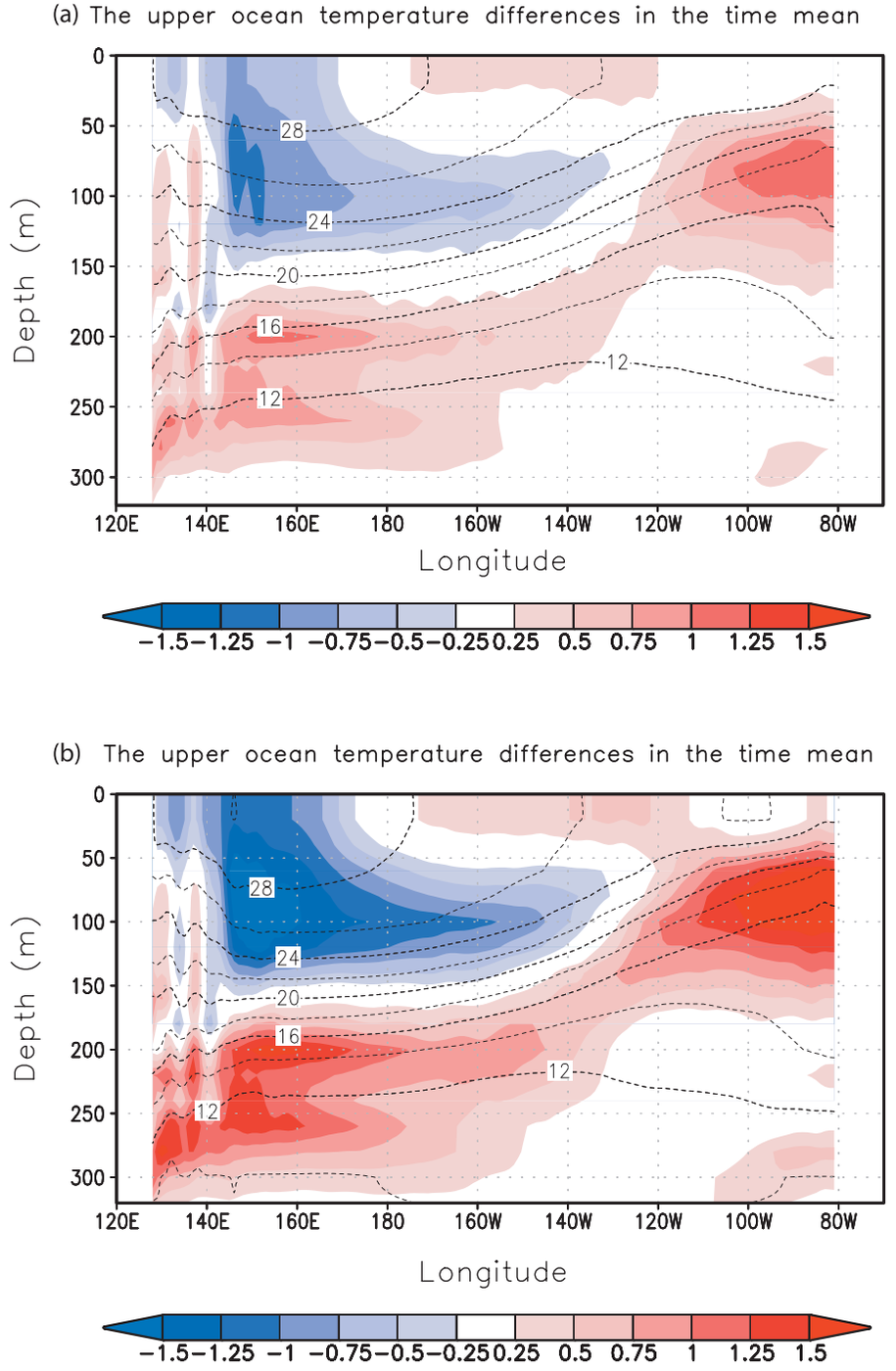

Plate 5. (a) Difference in the equatorial upper ocean temperature between the run with constant wind and the run with fluctuating wind. (b) Same as Plate 5a except the fluctuation part of the wind is amplified by 50%.

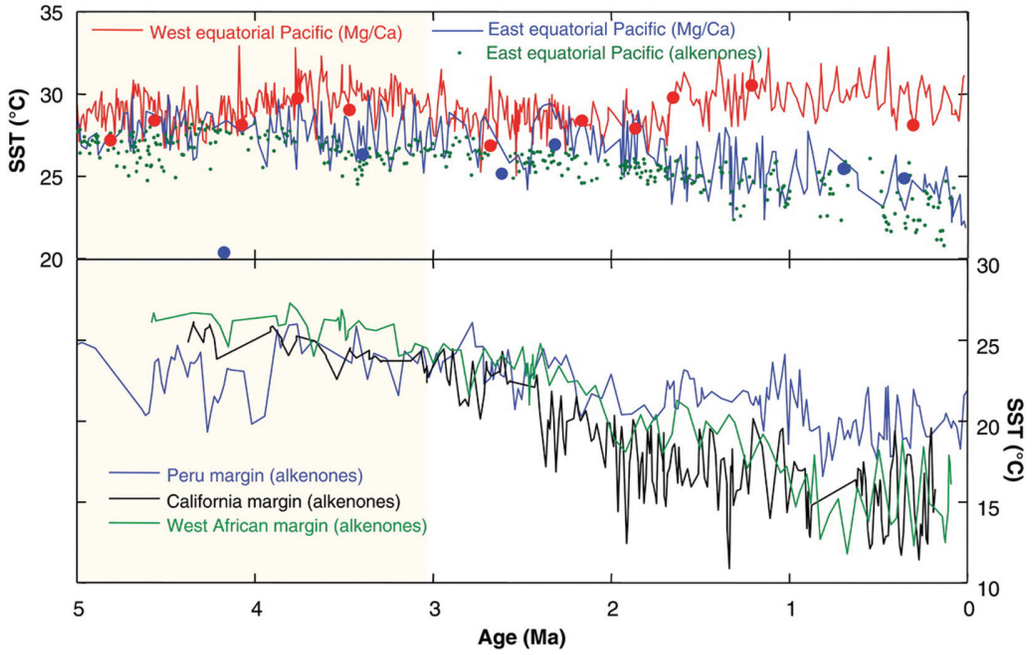

Plate 6. (top) SST records in the western equatorial Pacific (red) and in the eastern equatorial Pacific (blue and green). (bottom) Alkenone-based SST records for the California margin (black), the Peru margin (blue), and the West African margin (green). From *Fedorov et al.* [2006]. Reprinted with permission from AAAS.

equatorial eastern Pacific). This scenario may serve as a useful null hypothesis in understanding the response of ENSO to global warming.

3. RECENT ELEVATION OF ENSO ACTIVITY

The recent elevation of ENSO activity over the last few decades offers a test of the relevance of the aforementioned theoretical results. Niño 3 SST anomalies in the instrumental record, together with its variance calculated using a moving window with a width of 16 years, are shown in Figure 7. The level of ENSO activity, measured by the variance on the decadal time scale, exhibits an upward trend over the last century. The trend is particularly impressive in the most recent three decades. The elevation of ENSO activity over the last 30 years is also evident in the variability in the subsurface temperature of the equatorial Pacific. Figure 8a shows the subsurface temperature anomalies in the eastern and western Pacific, and Figure 8b is the difference between the two. ENSO involves a zonal redistribution of equatorial upper ocean water, causing warming in the eastern upper ocean and cooling in the subsurface of the western Pacific. Thus the difference between the subsurface temperature in these two regions is arguably a more complete measure of the ENSO activity.

Is this elevation consistent with the theory developed in the previous sections? Figure 9a shows the time series of tropical maximum SST (which may be regarded as the T_w in the analytical model) that corresponds to the Niño 3 SST time series in Figure 7. Overall, the trend over the last century is positive, but the rate of increase over the past three decades or so is particularly impressive. This rapid increase in the value of T_w corresponds to the elevated ENSO activity as shown in Figure 7. Figure 9b shows the global distribution of SST trend over the last three decades. Note that while the warm pool SST has been increasing, the corresponding trend in the eastern equatorial Pacific is negative. So the last 30 years corresponds to a period with a strengthening zonal SST contrast. Consistent with the negative trend in the eastern equatorial Pacific, the subsurface of the equatorial eastern Pacific and the connected thermocline water temperature (T_c) also have a negative trend (Figure 10). Clearly, the difference between the warm pool SST and the temperature of the equatorial thermocline water ($T_w - T_c$) over the last three decades or so has been increasing. So the relationship between the tendency in T_w and T_c and the anomalous activity of ENSO in this period is consistent with the theoretical prediction.

Will the elevated ENSO activity be likely to continue? Figure 11 shows the time series of $T_w - T_c$. As indicated by

this stability measure, the coupled system is clearly less stable than the previous decades. There is not yet a clear hint from this time series that this elevation in $T_w - T_c$ is beginning to wane. So we expect the anomalous activity of ENSO is likely to continue into the coming decades.

4. ENSO IN THE PAST CLIMATES

Proxy data about the behavior of the past climates offer more opportunities to test the relevance of our theoretical results. One finding concerning the behavior of ENSO in the past climates is that it has a long history, a continuing presence up to 3 million years ago [*Fedorov et al.*, 2006]. The collateral question is why it did not exist before then. An examination of the evolution of the zonal SST contrast indicates that the birth of ENSO corresponds to a time when the zonal SST contrast reaches a substantial value (Plate 6) [*Wara et al.*, 2005]. Figure 7 shows the proxy SST records for the tropical Pacific over the last 5 millions years. Before about 3 million years ago, the high latitudes were considerably warmer [see *Fedorov et al.*, 2006, Figure 1]. This high-latitude warmth may result in much warmer upwelling water in the equatorial zone, a much weakened zonal SST contrast (see Plate 7), and consequently the disappearance of ENSO (or a permanent El Niño condition) (recall Figure 3).

While ENSO is believed to have a 3 million year long continuing history, its level of activity has varied, at least in the last 1500 years [*Moy et al.*, 2002; *Cobb et al.*, 2003; *Rein et al.*, 2004; *Rein*, 2005; *Graham et al.*, 2007; *Newton et al.*, 2006; *Mann et al.*, 2009; *Sachs et al.*, 2009]. Of particular interest in the present context are those centennial-scale changes that correspond to the so-called Medieval Climate Anomaly and the Little Ice Age (LIA), periods during which distinct climate changes were also registered in the extratropical regions [*Crowley and Lowery*, 2000; *Bradley et al.*, 2003; *Mann et al.*, 2009; *Graham et al.*, 2007; *Trouet et al.*, 2009].

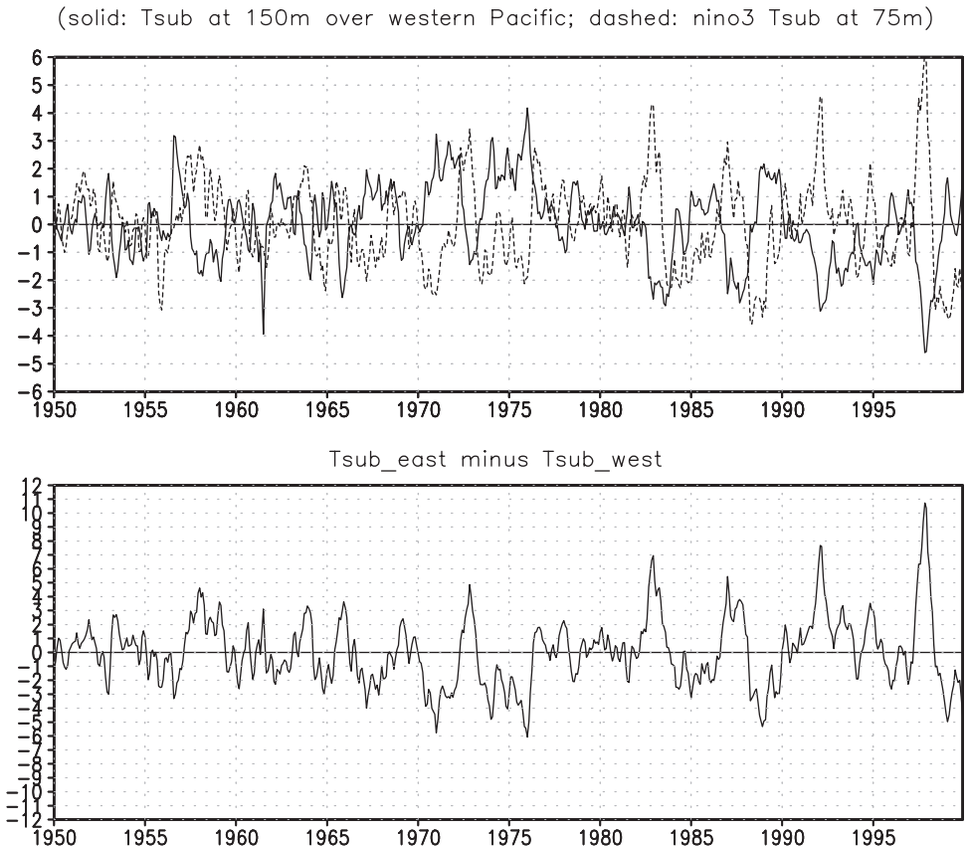

Figure 8. (top) Time series of the subsurface temperature in the equatorial eastern Pacific (90°W–150°W, 5°S–5°N, 75 m) (dashed line) and the subsurface temperature in the western Pacific (130°E–170°E, 5°S–5°N, 150 m) (solid line). (bottom) Difference between the two temperatures.

The proxy data by *Rein et al.* [2004] suggests weak ENSO activity during the Medieval Warm Period (MWP) (Figure 12). This finding is also supported by the inferred mean climate change during this period, which is La Niña–like (Pacific [*Cobb et al.*, 2003; *Graham et al.*, 2007; *Conroy et al.*, 2008; *Oppo et al.*, 2009; *Mann et al.*, 2009]). The relationship between the mean state change and the level of ENSO activity exhibited in the instrumental record of the last 50 years is that an El Niño–like change in the mean state be accompanied by a higher level of ENSO activity and a La Niña change in the mean state be accompanied by a lower level of ENSO activity [*Zhang et al.*, 1997; *Vecchi et al.*, 2008]. Such a relationship between the mean state and the level of ENSO activity is consistent with the observed asymmetry between the two

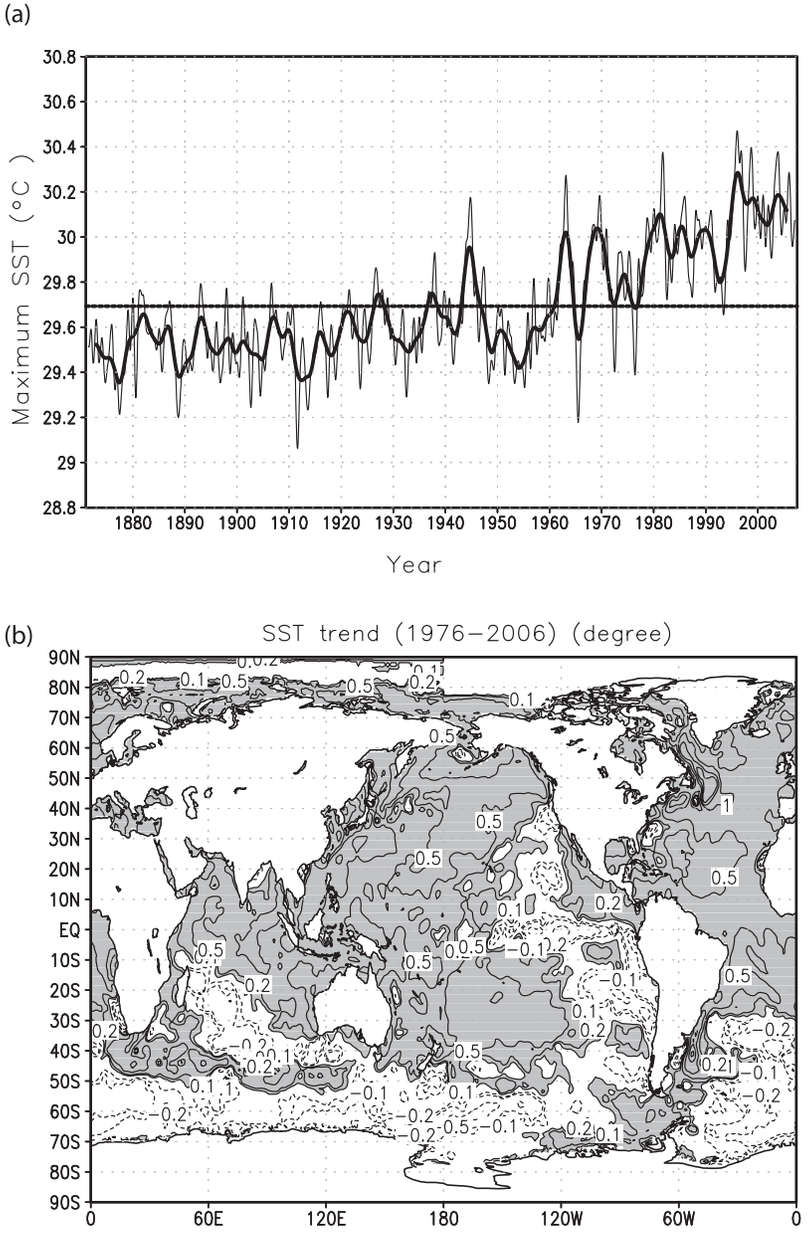

Figure 9. (a) Time series of tropical maximum SST that corresponds to the Niño 3 SST time series shown in Figure 7. (b) Spatial distribution SST trends over the last three decades (1976–2006). Areas with positive trends are shaded.

phases of ENSO: El Niño, on average, is stronger than La Niña, so stronger ENSO activity translates into El Niño–like changes in the mean state [*Zhang et al.*, 2009].

With regard to the LIA, the recent finding by *Cobb et al.* [2003] suggests that the level of ENSO activity during the LIA is relatively strong (Plate 8). The inference for an elevated ENSO activity during the LIA is also consistent with the finding of a southward movement of the Intertropical Convergence Zone by *Sachs et al.* [2009].

In light of the theoretical analysis in the previous sections, it is tempting to hypothesize that the relatively strong ENSO during LIA and the relatively weak ENSO during MWP are again responses to changes in the value of $T_w - T_c$, which occur over the centennial time scale in response to the changes in the pole to equator temperature difference.

5. POSSIBLE PROBLEMS WITH IPCC MODELS

The theoretical analysis and the paleodata suggest a sensitivity of ENSO to global climate change. State-of-the-art models, on the other hand, predict an almost muted response of ENSO to global warming. Early models with the use of flux adjustment predict a slight weakening of ENSO activity in response to global warming [*Knutson et al.*, 1997; *Meehl et al.*, 1993]. More recent models without the use of flux adjustment suggest even less sensitivity [*van Oldenborgh et al.*, 2005]. The lack of sensitivity to global warming was also noted in a simulation of Eocene climate [*Huber and Caballero*, 2003].

How do we possibly reconcile the gap between the theoretical results and the general circulation model (GCM) simulations of global warming? One possibility is that the models on which the theoretical analysis is based are too simple. We will return to this possibility in the last section of this chapter. The other possibility is that some relevant processes are still inadequately represented in the state-of-the-art climate models. Indeed, while there are general improvements in the models used for the IPCC's Fourth Assessment Report compared to their earlier versions [*AchutaRao and Spencer*, 2006], they still have errors in reproducing the observed ENSO events [*Guilyardi et al.*, 2009]. Of particular relevance to the theoretical results in the present chapter is the asymmetry of ENSO, an aspect whose representation in the climate models may be particularly problematic. The variance

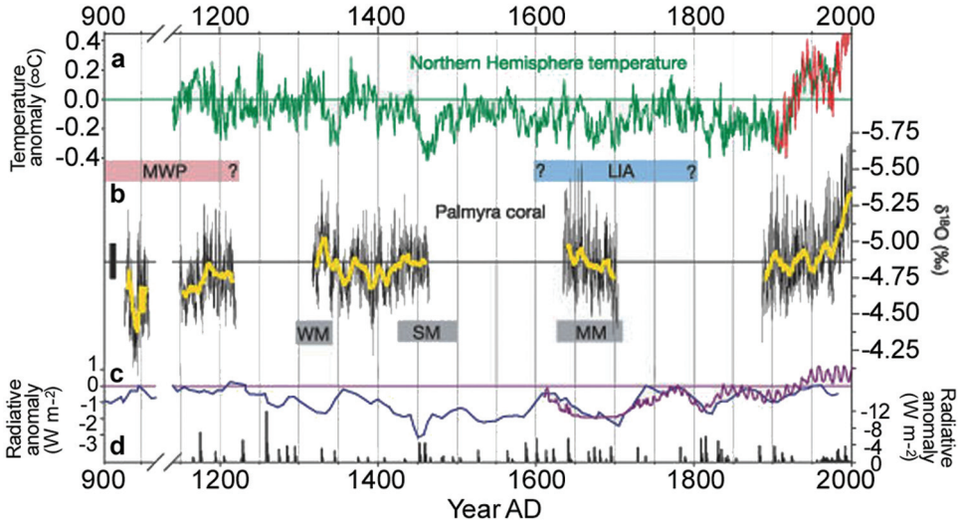

Plate 7. (a) Northern Hemisphere temperature reconstruction by *Mann et al.* [1998] (green) plotted with the Northern Hemisphere instrumental temperature record (red). The green horizontal line denotes the mean of the MBH record for the period A.D. 1886–1975. (b) Monthly resolved Palmyra coral ^{18}O records (thin black line), shown with a 10 year running average (thick yellow line). The black horizontal line represents the average of the Palmyra modern coral ^{18}O for the period A.D. 1886–1975. (c) Reconstruction of solar irradiance anomalies based on historical sunspot records (anomalies calculated with respect to the A.D. 1886–1975 mean) (purple) plotted with ^{10}Be anomalies (a proxy for solar activity) (blue), plotted as a three-point running mean and scaled to the solar irradiance anomalies. (d) Radiative forcing associated with volcanic eruptions recorded in ice cores (black). The approximate timing and duration of the Little Ice Age (LIA), the Medieval Warm Period (MWP), and solar activity minima, the Maunder minimum (MM), the Spörer minimum (SP), and the Wolfe minimum (WM), are marked by horizontal bars. From *Cobb et al.* [2003].

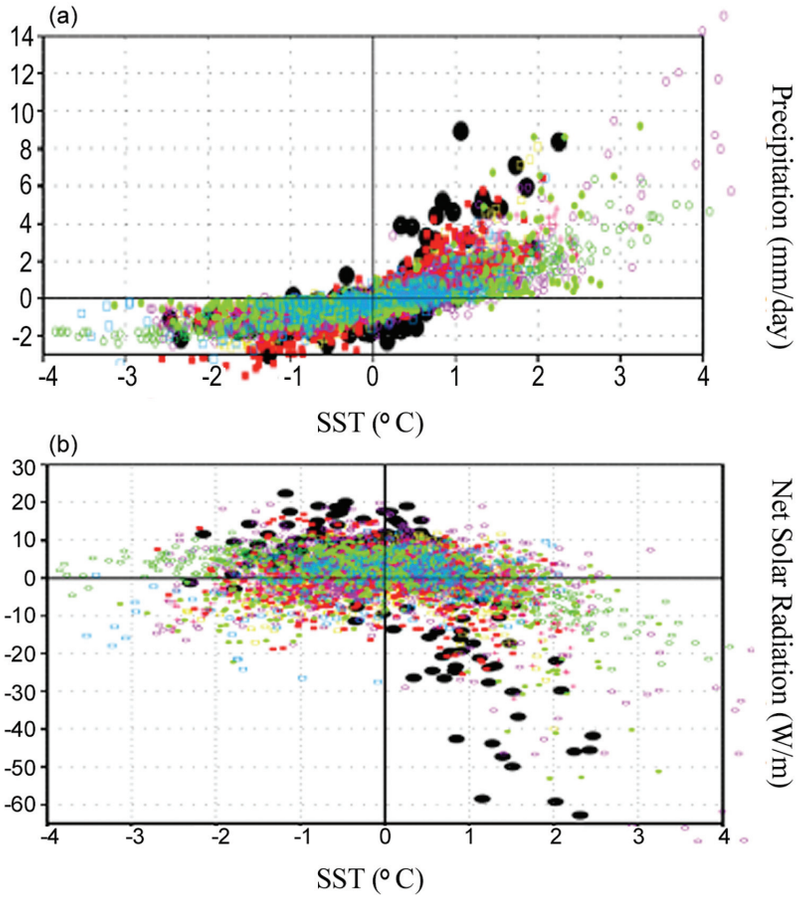

Plate 8. Scatter diagrams showing the relationship (a) between SST and precipitation and (b) between SST and the cloud albedo. Data are interannual anomalies averaged over the equatorial Pacific (150°E–250°E, 5°S–5°N). The color dots are for the various models, and the black dotes are for the real world (see *Sun et al.* [2009] for more details).

of Niño 3 SST has been commonly used to measure the level of ENSO activity, but the asymmetry in the simulated ENSO may not correlate with the variance of Niño 3 SST. Figure 13a illustrates this point using the various versions of the NCAR Community Climate System Model (CCSM) as an example. Figure 13a shows that while the variance of the Niño 3 SST in the later versions of NCAR CCSM is comparable or even exceeds that from the observations, the skewness of the Niño 3 SST is still far too weak (Figure 13a). This is also true for the subsurface temperature of the equatorial eastern Pacific (Figure 13b). The more symmetric ENSO in the models suggest that the processes that give rise to "ENSO" in the models may be too linear.

The precipitation-SST relationships in the models are indeed more linear in the models than in the observations. Plate 8a shows the relationship between precipitation and SST during ENSO over the equatorial Pacific in the observations and models. Plate 8a shows that the observed SST and precipitation have a rather nonlinear relationship: the rate of increase of precipitation with SST picks up quickly once the SST exceeds its climatological value (i.e., near the zero point as is plotted here). The corresponding relationship in the models, in contrast, is more linear. Consequently, measured about their respective climatology, the precipitation increases with SST increase at a faster rate in the observations than those in the models. Only when the positive SST anomalies are very large, does the rate of increase of precipitation with respect to SST in some models become more comparable to that in the observations. Plate 8b shows that the relationship between the surface solar radiation and SST mirrors the relationship between precipitation and SST. About its respective climatology, the surface solar radiation decreases at a faster

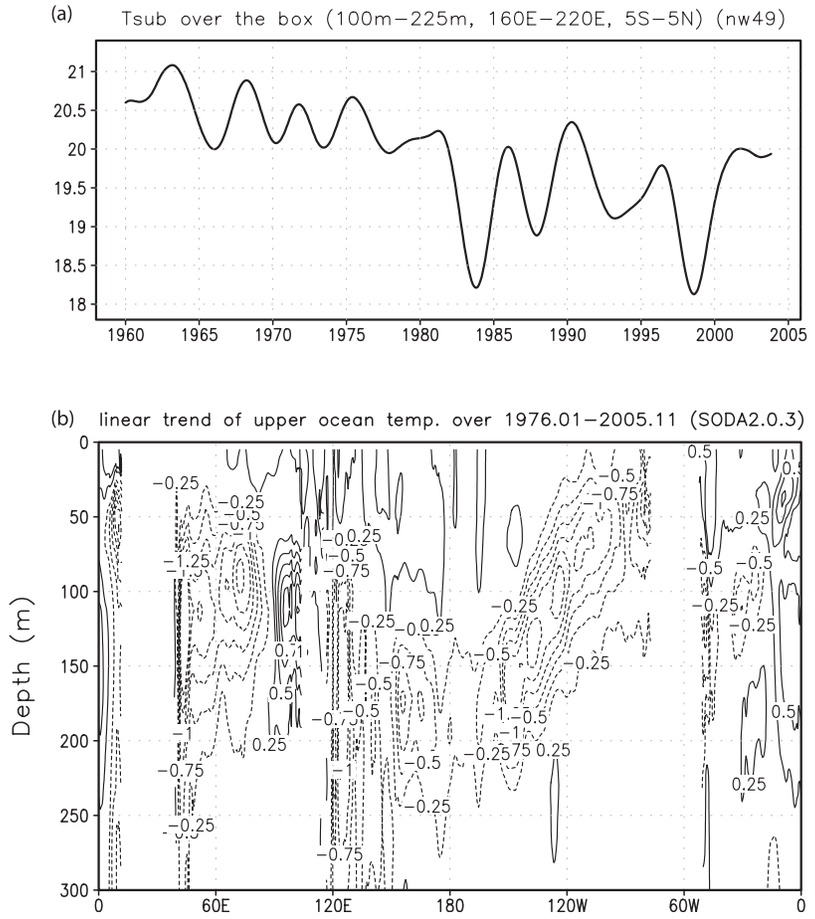

Figure 10. (a) Time series of T_c, defined here as the average equatorial subsurface temperature in the region (100–225 m, 160°E–220°E, 5°S–5°N). (b) Trend in the equatorial upper ocean temperature over the last 30 years.

rate in the observations than in the models. Clearly, measured either by the precipitation that deep convection produces, or by its reflectivity of solar radiation, deep convection in the observations responds more sensitively and more nonlinearly than in the models. *Zhang et al.* [2009] show that the improved ENSO asymmetry in the NCAR CCSM3.5 [*Neale*

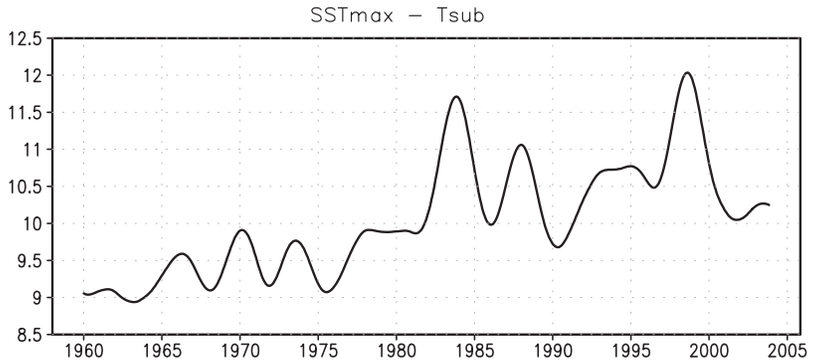

Figure 11. Evolution of $T_w - T_c$ over the last 50 years. Note the elevated state in the last 30 years.

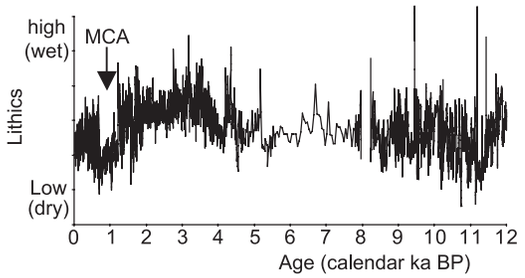

Figure 12. Down-core lithic concentrations at site 106 KL. MCA is Medieval Climate Anomaly. From *Rein et al.* [2004].

et al., 2008] is likely due to an improvement in the precipitation-SST relationship in the model. More studies are needed to address the full extent of the impact of a less responsive deep convection to SST increases on the response of the tropical climate to anthropogenic forcing. It is tempting to suspect, however, that an inadequately responsive deep convection in the models may be responsible for the lack of sensitivity of ENSO to global warming in the simulations by IPCC models.

6. FINAL REMARKS

Motivated to better understand the response of ENSO to global warming, we have attempted to address the following two issues: (1) what the relationship between the amplitude of ENSO and the radiative heating is and (2) whether ENSO collectively constitutes an important feedback, which, in turn, may determine the mean state. Our results suggest that the level of ENSO activity (on decadal and longer time scales) may be proportional to the tendency in the temperature difference between the surface water in the western Pacific warm pool and the water constituting the equatorial undercurrent. Moreover, ENSO events may collectively act as a basin-scale heat mixer in the tropical Pacific that prevents the long-term mean value of the difference between the warm pool SST and the temperature of the equatorial undercurrent from exceeding a critical value. The finding points to a mechanism by which global warming influences ENSO. Specifically, our finding raises the following scenario for the response of ENSO to global warming: an elevated level of ENSO activity is likely to occur during the initial stages of global warming, but a reduced level of ENSO activity (or even a permanent El Niño state) is likely to ensue when global warming is full-blown. The trend in the level of ENSO activity in the instrumental record appears to be consistent with this scenario. The behavior of ENSO in the past climates also supports this prediction. However, coupled GCM simulations fail to produce this scenario. It is suggested that an inadequate sensitivity of the tropical hydrological cycle in the models to SST changes due to a lack of strong nonlinearity in the deep convection–SST relationship may be responsible for the lack of response in the level of ENSO activity to global warming.

We would like to highlight some potential caveats in the theoretical results we have highlighted in this chapter. First, the results so far have been based on models that do not have the stochastic forcing from weather events. A significant role of stochastic forcing from weather events in the dynamics of ENSO has been suggested by a number of studies [*Lau*, 1985; *Kleeman and Power*, 1994; *Penland and Sardeshmukh*, 1995; *Chang et al.*, 1996; *Wang et al.*, 1999; *Kessler and Kleeman*, 2000]. A particular illuminating result from these studies is that the irregularity in ENSO may be more easily explained as the presence of stochastic forcing rather than a consequence of chaotic dynamics. These studies, the linear inversed models of ENSO in particular, also suggest a role for the magnitude of the stochastic forcing from the weather events in determining the average magnitude ENSO. Thus, further studies need to include the stochastic aspects of the weather events. However, as the magnitude of the stochastic forcing from the weather events is likely dependent on the warm pool SST, we expect that this additional forcing of ENSO should enhance the response of ENSO to global warming in the initial stage. Whether the enhanced weather forcing could outweigh the stabilizing effect from a reduced $T_w - T_c$ in the later stage of global warming is clearly an enticing question for further investigation.

Another aspect that could complicate the proposed picture is the annual cycle, a factor we have not been able to include in a realistic way in our theoretical models. ENSO is phase-locked to the annual cycle [*Rasmusson and Carpenter*, 1982]. While why this is so remains to be fully understood [*Tziperman*, 1997; *Cane*, 2004], the response of ENSO to global warming may depend on the response of the annual cycle to global warming. Indeed, *Clement et al.* [1996] interpreted the response of ENSO to a uniform increase in the radiative heating in the Z-C model in terms of the seasonal dependence of the growth rate of SST anomalies. An interesting feature of the Z-C model is that in response to a uniform increase in the restoring SST (equivalent to an increase in the tropical maximum SST as given by *Sun* [1997]), the zonal SST contrast increases but the level of ENSO activity does not [*Clement et al.*, 1996; *Cane et al.*, 1997] (Figure 14). The latter result differs from that of *Sun* [1997]. *Sun* [1997] suggested that the difference in the treatment of the subsurface temperature response to the increase in the surface heating could explain the difference in the response of ENSO amplitude. The subsequent studies of

Sun [2003], *Sun et al.* [2004], and *Sun and Zhang* [2006] further underscore this possibility. However, the substantial variability in the level of ENSO activity on the decadal, centennial, and longer time scale in the Z-C model also makes the inference of the response to an increase in the external heating a more involved issue. What is sure for now is that more studies are also needed to reconcile the results among simple models.

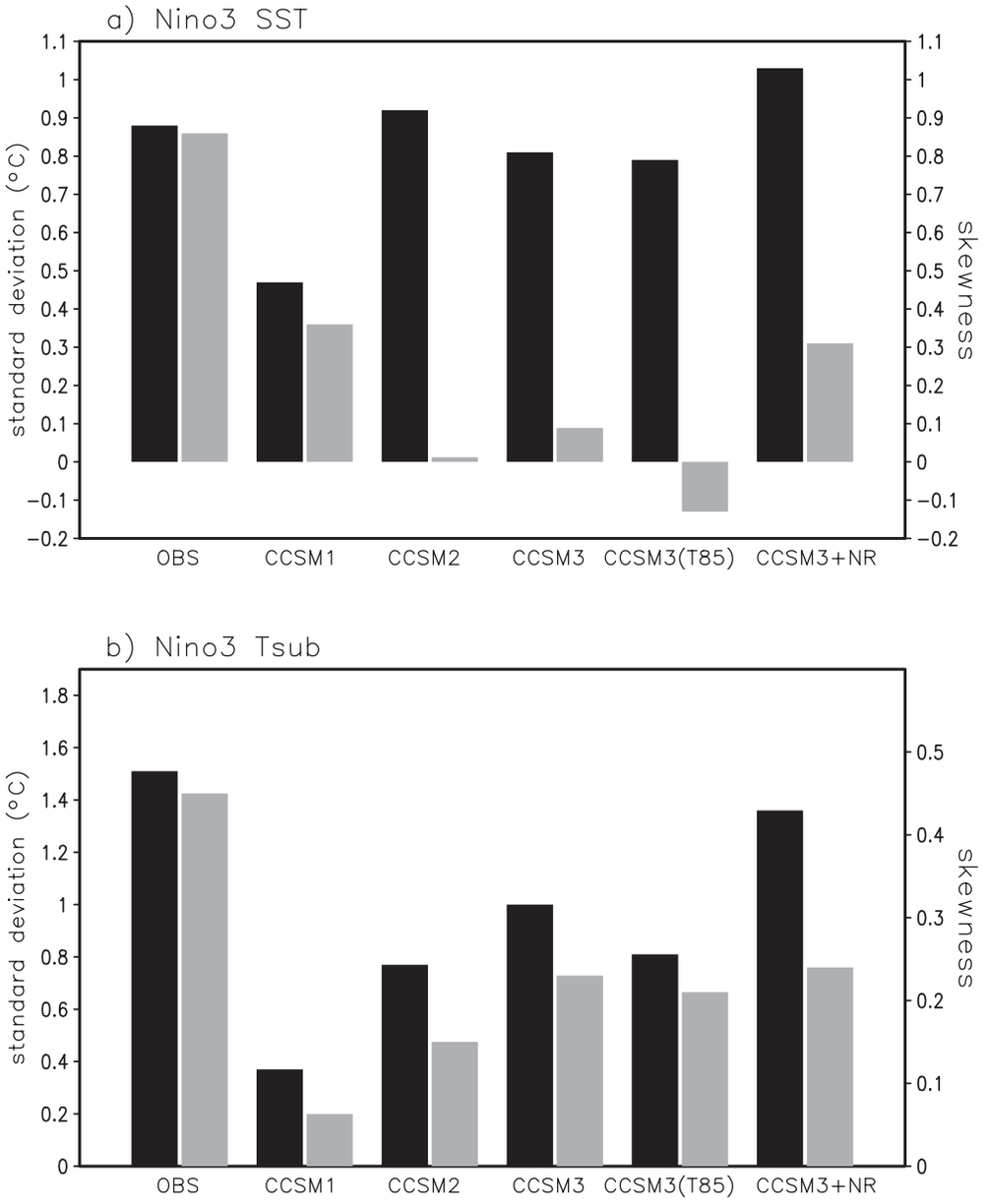

Figure 13. (a) Standard variations (black) and skewness (gray) of Niño 3 SST for observations and various versions of NCAR models. (b) Standard variations (black) and skewness (gray) of subsurface temperature in the eastern Pacific for observations and various versions of NCAR models. Note that although measured by the standard variations of Niño 3 SST, ENSO in the models is as strong or even stronger than the observations; ENSO is generally weaker in the models than in the observations measured by the variations of the subsurface SST. Measured by skewness, ENSO is weaker in all models, whether viewed at the surface or the subsurface.

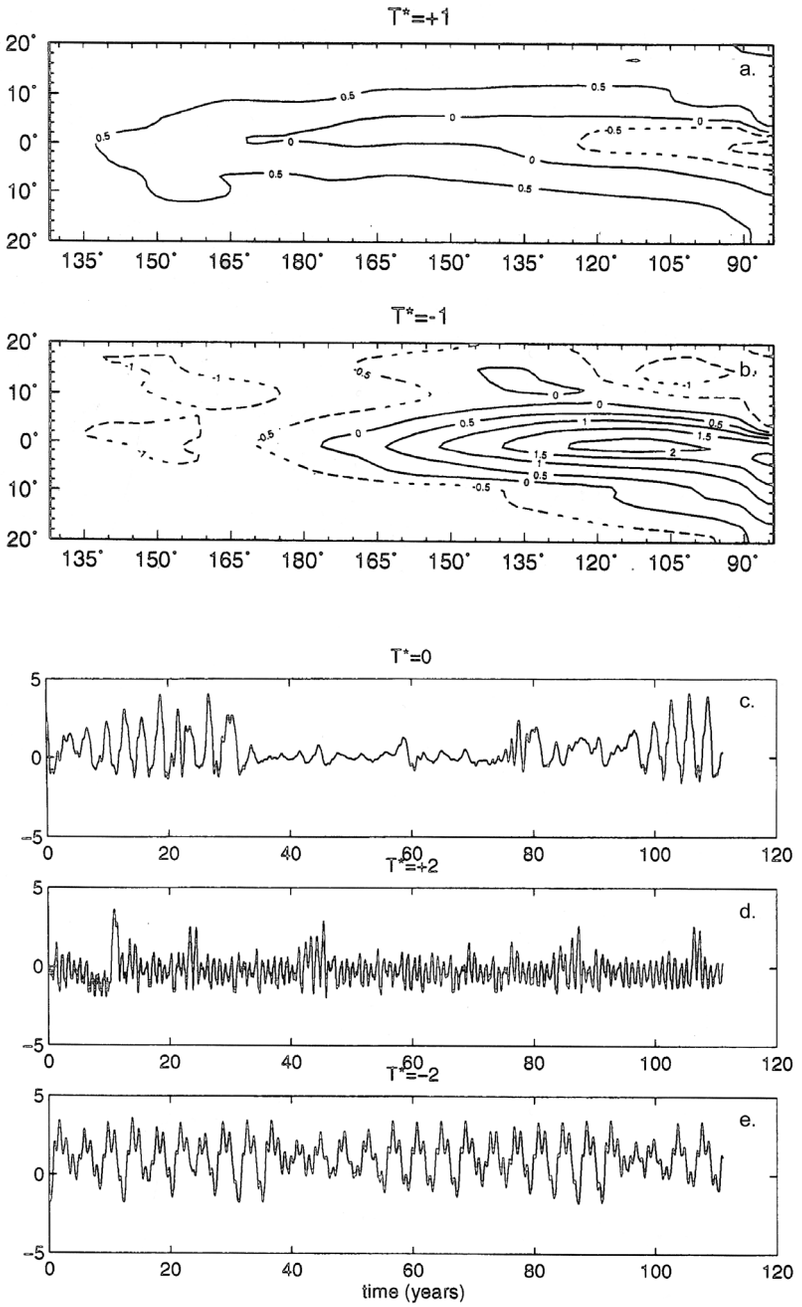

Figure 14. (a) Response in the mean SST to a 1 K increase in the restoring SST. (b) Response in the mean to a 1 K decrease in the restoring SST. (c) Time series of Niño 3 SST from a control run. (d) Time series of Niño 3 SST when the restoring SST is increased by 2 K. (e) Time series of Niño 3 SST when the restoring SST is lowed by 1 K. From *Clement et al.* [1996].

Acknowledgments. The work was supported by NOAA's Global Program and NSF's Large-Scale and Climate Dynamics Program and NSF's Physical Oceanography Program (ATM-9912434, ATM-0331760, ATM-0852329, and ATM-0553111). The author would like to thank Tao Zhang and Yongqiang Yu for their help in the research.

REFERENCES

AchutaRao, K., and K. R. Sperber (2006), ENSO simulation in coupled ocean-atmosphere models: Are the current models better?, *Clim. Dyn.*, *27*, 1–15.

Barsugli, J. J., J. S. Whitaker, A. F. Loughe, P. D. Sardeshmukh, and Z. Toth (1999), Effect of the 1997/98 El Niño on individual large-scale weather events, *Bull. Am. Meteorol. Soc.*, *80*, 1399–1412.

Bradley, R. S., M. K. Hughes, and H. F. Diaz (2003), Climate in medieval time, *Science*, *302*, 404–405.

Cane, M. A. (2004), The evolution of El Niño, past and future, *Earth Planet. Sci. Lett.*, *164*, 1–10.

Cane, M. A., A. C. Clement, A. Kaplan, Y. Kushnir, D. Poznyakov, R. Seager, S. E. Zebiak, and R. Murtugudde (1997), Twentieth-century sea surface temperature trends, *Science*, *275*, 957–960.

Cayan, D. R., K. T. Redmond, and L. G. Riddle (2000), ENSO and hydrological extremes in the western United states, *J. Clim.*, *12*, 2881–2893.

Chang, P., L. L. Ji, H. Li, and M. Flügel (1996), Chaotic dynamics versus stochastic processes in El Niño-Southern Oscillation in coupled ocean-atmosphere models, *Physica D*, *98*, 301–320.

Clement, A., R. Seager, M. A. Cane, and S. E. Zebiak (1996), An ocean dynamical thermostat, *J. Clim.*, *9*, 2190–2196.

Cobb, K. M., C. D. Charles, H. Cheng, and R. L. Edwards (2003), Coral records of the El Niño-Southern Oscillation and tropical pacific climate over the last millennium, *Nature*, *424*, 271–276.

Conroy, J. L., A. Restrepo, J. T. Overpeck, M. Steinitz-Kannan, J. E. Cole, M. B. Bush, and P. A. Colinvaux (2008), Unprecedented recent warming of surface temperatures in the eastern tropical Pacific Ocean, *Nat. Geosci.*, *2*, 46–50, doi:10.1038/ngeo390.

Crowley, T. J., and T. S. Lowery (2000), How warm was the Medieval Warm Period?, *Ambio*, *29*, 51–54.

Deser, C., M. A. Alexander, and M. Timlin (1996), Upper ocean thermal variations in the North Pacific during 1970–1991, *J. Clim.*, *9*, 1840–1855.

Fedorov, A. V., P. S. Dekens, M. McCarthy, A. C. Ravelo, P. B. deMenocal, M. Barreiro, R. C. Pacanowski, and S. G. Philander (2006), The Pliocene paradox (mechanisms for a permanent El Niño), *Science*, *312*, 1485–1489.

Gent, P. R., and M. A. Cane (1989), A reduced gravity, primitive equation model of the upper equatorial ocean, *J. Comput. Phys.*, *81*, 444–480.

Glantz, M. H. (2001), *Currents of Change: Impacts of El Niño and La Niña on Climate and Society*, 252 pp., Cambridge Univ. Press, New York.

Graham, N. E., et al. (2007), Tropical Pacific—Mid-latitude teleconnections in medieval times, *Clim. Dyn.*, *83*, 241–285.

Guilyardi, E., A. Wittenberg, A. Fedorov, M. Collins, C. Wang, A. Capotondi, G. J. van Oldenborgh, and T. Stockdale (2009), Understanding El Niño in ocean–atmosphere general circulation models: Progress and challenges, *Bull. Am. Meteorol. Soc.*, *90*, 325–340.

Hoerling, M. P., and A. Kumar (2003), The perfect ocean for drought, *Science*, *299*, 691–694.

Huang, R., and Y. Wu (1989), The Influence of ENSO on the summer climate change in China and its mechanism, *Adv. Atmos. Sci.*, *6*, 21–32.

Huber, M., and R. Caballero (2003), Eocene El Niño: Evidence for robust tropical dynamics in the "hothouse," *Science*, *299*, 877–881.

Intergovernmental Panel on Climate Change (2007), *Climate Change 2007: The Physical Science Basis: Working Group I Contribution to the Fourth Assessment Report of the IPCC*, edited by S. Solomon, et al., Cambridge Univ. Press, New York, (Available at http://www.ipcc.ch/ipccreports/ar4-wg1.htm).

Jin, F.-F. (1996), Tropical ocean-atmosphere interaction, the Pacific cold tongue, and the El Niño-Southern Oscillation, *Science*, *274*, 76–78.

Kessler, W. S. (2002), Is ENSO a cycle or a series of events?, *Geophys. Res. Lett.*, *29*(23), 2125, doi:10.1029/2002GL015924.

Kessler, W. S., and R. Kleeman (2000), Rectification of the Madden-Julian Oscillation into the ENSO cycle, *J. Clim.*, *13*, 3560–3575.

Kleeman, R., and S. B. Power (1994), Limits to predictability in a coupled ocean-atmosphere model due to atmospheric noise, *Tellus, Ser. A*, *46*, 529–540.

Knutson, T. R., S. Manabe, and D. Gu (1997), Simulated ENSO in a global coupled ocean-atmosphere model: Multidecadal amplitude modulation and CO_2 sensitivity, *J. Clim.*, *10*, 131–161.

Lau, K.-M. (1985), Elements of a stochastic-dynamical theory of the long-term variability of the El Niño/Southern Oscillation, *J. Atmos. Sci.*, *42*, 1552–1558.

Lin, J.-L. (2007), The double-ITCZ problem in IPCC AR4 coupled GCMs: Ocean-atmosphere feedback analysis, *J. Clim.*, *20*, 4497–4525.

Liu, Z., S. G. H. Philander, and R. C. Pacanowski (1994), A GCM study of tropical–subtropical upper-ocean water exchange, *J. Phys. Oceanogr.*, *24*, 2606–2623.

Lorenz, E. (1963), Deterministic nonperiodic flow, *J. Atmos. Sci.*, *20*, 131–141.

Mann, M. E., R. S. Bradley, and M. K. Hughes (1998), Global-scale temperature patterns and climate forcing over the past six centuries, *Nature*, *392*, 779–787, doi:10.1038/33859.

Mann, M. E., Z. Zhang, S. Rutherford, R. S. Bradley, M. K. Hughes, D. Schindell, C. Ammann, G. Faluvegi, and F. Ni (2009), Global signatures and dynamical origins of the Little Ice Age and medieval climate anomaly, *Science*, *326*, 1256–1260, doi:10.1126/science.1177303.

McPhaden, M. J., S. E. Zebiak, and M. H. Glantz (2006), ENSO as an integrating concept in Earth science, *Science*, *314*, 1740–1745.

McCreary, J. P., and P. Lu (1994), On the interaction between the subtropical and the equatorial oceans: The subtropical cell, *J. Phys. Oceanogr.*, *24*, 466–497.

Meehl, G. A., G. W. Branstator, and W. M. Washington (1993), Tropical Pacific interannual variability and CO_2 climate change, *J. Clim.*, *6*, 42–63.

Meehl, G. A., C. Covey, B. McAvaney, M. Latif, and R. J. Stouffer (2005), Overview of the Coupled Model Intercomparison Project, *Bull. Am. Meteorol. Soc.*, *90*, 89–93.

Moy, C. M., G. O. Seltzer, D. T. Rodbell, and D. M. Anderson (2002), Variability of El Niño/Southern Oscillation activity at millennial timescales during the Holocene epoch, *Nature*, *420*, 162–165.

Neale, R. B., J. H. Richter, and M. Jochum (2008), The impact of convection on ENSO: From a delayed oscillator to a series of events, *J. Clim.*, *21*, 5904–5924.

Neelin, J. D., D. S. Battisti, A. C. Hirst, F.-F. Jin, Y. Wakata, T. Yamagata, and S. E. Zebiak (1998), ENSO theory, *J. Geophys. Res.*, *103*, 14,261–14,290.

Newton, A., R. Thunell, and L. Stott (2006), Climate and hydrographic variability in the Indo-Pacific Warm Pool during the last millennium, *Geophys. Res. Lett.*, *33*, L19710, doi:10.1029/2006GL027234.

O'Brien, J. J., T. S. Richards, and A. C. Davis (1996), The effect of El Niño on U.S. landfalling hurricanes, *Bull. Am. Meteorol. Soc.*, *77*, 773–774.

Oppo, D. W., Y. Rosenthal, and B. K. Linsley (2009), 2000-year-long temperature and hydrology reconstructions from the Indo-Pacific Warm Pool, *Nature*, *460*, 1113–1116.

Pedlosky, J. (1987), An inertial theory of the equatorial undercurrent, *J. Phys. Oceanogr.*, *17*, 1978–1985.

Penland, C., and P. D. Sardeshmukh (1995), The optimal growth of tropical sea surface temperature anomalies, *J. Clim.*, *8*, 1999–2024.

Penland, C., D.-Z. Sun, A. Capotondiand , and D. J. Vimont (2010), A brief introduction to El Niño and La Niña, in *Climate Dynamics: Why Does Climate Vary?*, *Geophys. Monogr. Ser.*, doi:10.1029/2008GM000846, this volume.

Rasmusson, E., and T. Carpenter (1982), Variations in tropical sea surface temperature and surface wind fields associated with the Southern Oscillation/El Niño, *Mon. Weather Rev.*, *110*, 354–384.

Rein, B., A. Lückge, and F. Sirocko (2004), A major Holocene ENSO anomaly during the medieval period, *Geophys. Res. Lett.*, *31*, L17211, doi:10.1029/2004GL020161.

Rein, B., A. Lückge, L. Reinhardt, F. Sirocko, A. Wolf, and W.-C. Dullo (2005), El Niño variability off Peru during the last 20,000 years, *Paleoceanography*, *20*, PA4003, doi:10.1029/2004PA001099.

Ropelewski, C. F., and M. S. Halpert (1996), Quantifying the Southern Oscillation precipitation relationships, *J. Clim.*, *9*, 1043–1059.

Sachs, J. P., D. Sachse, R. H. Smittenberg, Z. Zhang, D. S. Battisti, and S. Golubic (2009), Southward movement of the Pacific intertropical convergence zone AD 1400–1850, *Nat. Geosci.*, *2*(7), 519–525.

Schneider, N., A. J. Miller, M. A. Alexander, and C. Deser (1999), Subduction of decadal North Pacific temperature anomalies: Observations and dynamics, *J. Phys. Oceanogr.*, *29*, 1056–1070.

Sun, D.-Z. (1997), El Niño: A coupled response to radiative heating?, *Geophys. Res. Lett.*, *24*, 2031–2034.

Sun, D. Z. (2000), Global climate change and El Niño: A theoretical framework, in *El Niño and the Southern Oscillation: Multiscale Variability and Global and Regional Impacts*, edited by H. F. Diaz and V. Markgraf, pp. 443–463, Cambridge Univ. Press, Cambridge, U. K.

Sun, D.-Z. (2003), A possible effect of an increase in the warm-pool SST on the magnitude of El Niño warming, *J. Clim.*, *16*, 185–205.

Sun, D.-Z. (2007), The Role of ENSO in regulating its background state, in *Nonlinear Dynamics in Geosciences*, edited by J. Elsner and A. Tsonis, pp. 537–555, Springer, New York.

Sun, D.-Z., and T. Zhang (2006), A regulatory effect of ENSO on the time-mean thermal stratification of the equatorial upper ocean, *Geophys. Res. Lett.*, *33*, L07710, doi:10.1029/2005GL025296.

Sun, D.-Z., T. Zhang, and S.-I. Shin (2004), The effect of subtropical cooling on the amplitude of ENSO: A numerical study, *J. Clim.*, *17*, 3786–3798.

Sun, D.-Z., et al. (2006), Radiative and dynamical feedbacks over the equatorial cold tongue: Results from nine atmospheric GCMs, *J. Clim.*, *19*, 4059–4074.

Sun, D.-Z., Y. Yu, and T. Zhang (2009), Tropical water vapor and cloud feedbacks in climate models: A further assessment using coupled simulations, *J. Clim.*, *22*, 1287–1304.

Timmermann, A., and F.-F. Jin (2002), A nonlinear mechanism for decadal El Niño amplitude changes, *Geophys. Res. Lett.*, *29*(1), 1003, doi:10.1029/2001GL013369.

Trenberth, K. E., G. W. Branstator, D. Karoly, A. Kumar, N.-C. Lau, and C. Ropelewski (1998), Progress during TOGA in understanding and modeling global teleconnections associated with tropical sea surface temperatures, *J. Geophys. Res.*, *103*, 14,291–14,324.

Trouet, V., J. Esper, N. E. Graham, A. Baker, J. D. Scourse, and D. C. Frank (2009), Persistent positive North Atlantic Oscillation Mode dominated the Medieval Climate Anomaly, *Science*, *324*, 78–80.

Tziperman, E. (1997), Mechanisms of seasonal-ENSO interaction, *J. Atmos. Sci.*, *54*, 61–71.

van Oldenborgh, G. J., S. Y. Philip, and M. Collins (2005), El Niño in a changing climate: A multi-model study, *Ocean Sci.*, *1*, 81–95.

Vecchi, G. A., A. Clement, and B. J. Soden (2008), Examining the tropical Pacific's response to global warming, *Eos Trans. AGU*, *89*(9), 81.

Wang, B., A. Barcilon, and Z. Fang (1999), Stochastic dynamics of El Niño–Southern Oscillation, *J. Atmos. Sci.*, *56*, 5–23.

Wang, B., J. Yang, T. Zhou, and B. Wang (2008), Interdecadal changes in the major modes of Asian–Australian monsoon variability: Strengthening relationship with ENSO since the late 1970s, *J. Clim.*, *21*, 1771–1789.

Wara, M. W., A. C. Ravelo, and M. L. Delaney (2005), Permanent El Niño-like conditions during the Pliocene warm period, *Science*, *309*, 758–761.

Zebiak, S. E., and M. A. Cane (1987), A model El Niño Southern Oscillation, *Mon. Weather Rev.*, *115*, 2262–2278.

Zhang, T., D.-Z. Sun, R. Neal, and P. J. Rasch (2009), An evaluation of ENSO asymmetry in the Community Climate System models: A view from the subsurface, *J. Clim.*, *22*, 5933–5961.

Zhang, Y., J. M. Wallace, and D. S. Battisti (1997), ENSO-like interdecadal variability, *J. Clim.*, *10*, 1004–1020.

D.-Z. Sun, Physical Science Division, Earth System Research Laboratory, NOAA, Boulder, CO 80303, USA. (dezheng.sun@noaa.gov)